

The Pennsylvania State University
The Graduate School
Department of Energy and Mineral Engineering

**Fe-MODIFIED ZSM-5 SHAPE SELECTIVE CATALYSTS FOR
THE SYNTHESIS OF 2, 6-DIMETHYLNAPHTHALENE**

A Thesis in
Energy and Geo-Environmental Engineering

by
Vasudha Dhar

© 2008 Vasudha Dhar

Submitted in Partial Fulfillment
of the Requirements
for the Degree of

Master of Science

May 2008

The thesis of Vasudha Dhar was reviewed and approved* by the following:

Chunshan Song
Professor of Fuel Science
Thesis Advisor

Sarma V. Pisupati
Associate Professor of Energy and Geo-Environmental Engineering

Andre L Boehman
Professor of Fuel Science and Materials Science and Engineering

Jonathan P. Mathews
Assistant Professor of Energy & Geo-Environmental Engineering
Graduate Program Chair

*Signatures are on file in the Graduate School

ABSTRACT

This work is a part of the DOE refinery Integration project at the Pennsylvania State University which involved the production of organic chemicals from coal blends and petroleum derived middle distillates as well as the production of advanced liquid fuels including diesel fuel, jet fuel and gasoline. The main objective of this work is to study metal modified zeolite catalysts to selectively improve the yield of 2, 6-dimethylnaphthalene during the alkylation of naphthalenes and methylnaphthalenes isolated from the coal blends and by products from petroleum refining operations like Light Cycle Oil (LCO) from the catalytic cracking unit. The major task in this application is to focus on the methylation of methylnaphthalene to get a higher selectivity of 2, 6-dimethylnaphthalene, an important feedstock for the 2, 6-naphthalenedicarboxylic acid, a precursor for the polymer polyethylene naphthalene (PEN). Since the key step is to achieve higher β - selectivity during the alkylation, 2-methylnaphthalene (2-MN) was taken as the model feed for the methylation in this work.

Medium pore zeolites were modified by the isomorphous substitution of Fe into the framework of the zeolites. The relative change in acidity based on the amount of Fe substitution in the zeolites was studied and its effect on the catalyst performance during the methylation reaction was studied. The changes in the catalyst properties after modification were studied using various characterization techniques. The reaction system was a fixed bed down flow reactor at 300°C at a WHSV of 6 h⁻¹. Prior to the experiments, the catalysts were pretreated *in-situ* at 450°C for one hour at atmospheric pressure under a nitrogen flow rate of 20 mL/min.

Several conclusions were drawn based on the methylation experiments on various catalysts and their characterization studies. The medium pore zeolite was found to exhibit β selectivity for this reaction but the conversion of 2-MN was reported to be very low for the catalyst. Also, a lot of secondary isomerization as well as non selective surface reactions were being carried out. The catalyst acidity also played a significant role in the selective formation of 2, 6-DMN. Based on the acidity studies using NH_3 -TPD and microcalorimetry, it was confirmed that the acidity of the catalysts was significantly lowered after modification. Based on the methylation reaction results, it was determined that the moderate acidity range gave the best 2, 6-DMN /2, 7-DMN ratio. Also it was found that the surface reactions were inhibited and this increased the overall 2, 6-DMN in the products.

The X-Ray diffraction studies revealed increase in the crystallinity of the modified samples confirming dealumination and a slight increase in the lattice parameters of the modified samples concurring with the Framework IR studies and ^{27}Al MAS NMR studies. However, no significant pore size changes were observed during modification with Fe. Further study is recommended do determine the effects of slight pore size alteration on the shape selective formation of the 2, 6-DMN.

Table of Contents

List of Figures.....	viii
List of Tables.....	xi
Acknowledgements.....	xiii
1 Introduction.....	1
2 Literature Review.....	4
2.1 Industrial processes for 2, 6-dimethylnaphthalene.....	4
2.2 Selective Production of 2, 6-DAN.....	9
2.2.1 Zeolites.....	11
2.2.2 Shape Selectivity in Zeolites.....	13
2.2.2.1 Zeolite Y.....	17
2.2.2.2 Mordenite.....	18
2.2.2.3 ZSM -5.....	18
2.3 Alkylation of Naphthalene.....	19
2.3.1 Isopropylation of Naphthalene.....	20
2.3.2 Methylation of Methylnaphthalene.....	22
2.3.3 Pathways for Shape Selective Methylation.....	26
2.4 Catalyst Modification Processes.....	29
2.4.1 External Surface Neutralization.....	29
2.4.2 Modification by Isomorphous Substitution.....	30
2.5 Application of Literature Concepts to the Hypothesis.....	31

3	Experimental.....	33
3.1	Catalyst Preparation.....	33
3.2	Catalyst characterization.....	35
3.2.1	Element Analysis by ICP –AES.....	35
3.2.2	Surface Area Measurements.....	36
3.2.3	X Ray Diffraction Studies.....	37
3.2.4	Nuclear Magnetic Resonance.....	37
3.2.5	Infrared Spectroscopy.....	38
3.2.6	Acidity Studies.....	38
3.2.6.1	Microcalorimetric Studies.....	39
3.2.6.2	Temperature Programmed Desorption.....	40
3.3	Catalyst Evaluation in Methylation Experiments.....	41
3.3.1	Feedstock Composition.....	41
3.3.2	Reactor System.....	42
3.3.3	Reaction Conditions.....	43
3.3.4	Sample Collection and Analysis.....	44
4	Results and Discussions.....	46
4.1	Preliminary Methylation Reactions.....	47
4.1.1	Effect of the Catalyst Type.....	47
4.1.2	Effect of the Temperature.....	51
4.1.3	Effect of SiO ₂ /Al ₂ O ₃ Ratio.....	53
4.2	Catalyst Characterization.....	55
4.2.1	Element Analysis by ICP –AES.....	55

4.2.2	X Ray Diffraction Studies.....	56
4.2.3	Surface Area Measurements.....	59
4.2.4	Infrared Spectroscopy.....	61
4.2.5	Nuclear Magnetic Resonance.....	62
4.2.6	Acidity Studies.....	64
4.2.6.1	Temperature Programmed Desorption (NH ₃).....	64
4.2.6.2	Microcalorimetric Studies.....	66
4.3	Effect of the Catalyst Modification on Methylation Reaction.....	71
4.4	Experimental Uncertainty.....	78
5	Summary, Conclusions and Recommendations for Future Work.....	81
5.1	Summary.....	82
5.2	Conclusions.....	83
5.3	Recommendations for Future Work.....	83
	References.....	85
	Appendix.....	90

LIST OF FIGURES

Figure 2.1 Flow diagram of BP Amoco 2, 6 NDC process from Lilliwitz LD; 2001.....	4
Figure 2.2 B.P Amoco's naphthalene carbonylation process from Lilliwitz L.D.; 2001...	6
Figure 2.3 MGC carbonylation process from Abe T. et al.; 1991.....	7
Figure 2.4 Schematic of Naphthalene Alkylation from Song C.; 2000.....	9
Figure 2.5 Examples of Bronsted acid and Lewis acid sites in the zeolite framework....	13
Figure 2.6 Reactant shape selectivity in alcohol dehydration reactions from Song C.; 2000.....	14
Figure 2.7 Product Shape Selectivity in the methylation of toluene from Song C.; 2000.....	15
Figure 2.8 Transition Shape selectivity in m-Xylene disproportionation reaction from Song C. et al. ; 2000.....	16
Figure 2.9 Crystalline structure of Y zeolite (Dimensions in Å) from Baerlocher C. et al.; 2001.....	17
Figure 2.10 Crystalline structure of Mordenite (Dimensions in Å) from Baerlocher C. et al.; 2001.....	18

Figure 2.11 Crystalline structure of Mordenite (Dimensions in Å) from Baerlocher C. et al.; 2001.....	19
Figure 2.12 Schematic of alkylation of naphthalene from Song, 2000.....	20
Figure 2.13 Reaction Pathways for methylation of 2 – methylnaphthalene from Komatsu T. et al.; 2000.....	27
Figure 3.1 Picture of the flow reactor system.....	43
Figure 4.1 Conversion Vs TOS for the methylation of 2MN at 300 at 6.0h ⁻¹ WHSV.....	49
Figure 4.2 Selectivity Vs TOS for the methylation of 2MN at 300°C at 6.0h ⁻¹ WHSV...	49
Figure 4.3 Conversion Vs TOS for the methylation of 2MN using CBV 5524G as a catalyst at 6.0h ⁻¹ WHSV.....	52
Figure 4.4: Selectivity Vs TOS for the methylation of 2MN using CBV 5524G as a catalyst at 6.0h ⁻¹ WHSV.....	52
Figure 4.5 Conversion Vs TOS for the methylation of 2MN at 300°C at 6.0h ⁻¹ WHSV..	54
Figure 4.6: Selectivity Vs TOS for the methylation of 2MN at 300°C at 6.0h ⁻¹ WHSV..	54
Figure 4.7 XRD Profiles of parent and modified samples.....	59
Figure 4.8: Framework IR spectra of the HZSM 5(Red) and Fe ZSM 5 2(Black) samples.....	62

Figure 4.9: ^{27}Al MAS NMR for the parent and modified zeolites.....	63
Figure 4.10: Si^{29} MAS NMR for the parent and modified zeolites.....	65
Figure 4.11: TPD profiles of Parent and modified catalyst samples.....	66
Figure 4.12: Differential Heats distribution of all the catalyst samples.....	69
Figure 4.13 Acidity spectra of the modified samples.....	70
Figure 4.14: 2 MN Conversion vs. TOS for the methylation of 2MN at 300°C at 6.0h ⁻¹ WHSV.....	73
Figure 4.15: Selectivity Vs TOS for the methylation of 2-MN at 300°C at 6.0h ⁻¹ WHSV.....	74
Figure 4.16: 2 MN Conversion vs. TOS for the methylation of 2MN at 300°C at 6.0h ⁻¹ WHSV.....	74
Figure 4.17: Selectivity Vs TOS for the methylation of 2-MN at 300°C at 6.0h ⁻¹ WHSV.....	75
Figure 4.18 Trend for 2, 6-DMN yield and 2, 6-DMN/2, 7-DMN ratio for methylation experiments.....	76
Figure 4.19 Conversion Vs TOS for three sets of duplicate experiments.....	80
Figure 4.20 2, 6-DMN/ 2, 7-DMN vs TOS (h) for three sets of duplicate experiments....	80

LIST OF TABLES

Table 3.1: Properties of the zeolites, as received.....	33
Table 3.2: Composition of the salts added in the slurry for each modified sample.....	35
Table 4.1 The DMN product distribution of the 2MN methylation reaction at 300°C and 6.0h ⁻¹ WHSV. (a = Pu S.B and Inui T.; 1996).....	50
Table 4.2: Chemical Composition of the catalyst samples before and after modification.....	56
Table 4.3: Crystallinity and lattice parameters of the samples.....	58
Table 4.4 Surface Area data for the modified samples.....	60
Table 4.5 Temperatures at the TPD peaks shown in the figure 4.11	65
Table 4.6 Acid strength distribution of parent and modified zeolites.....	67
Table 4.7 Product distribution of DMN's during methylation reaction conducted using Fe modified catalysts.....	75
Table 4.8 Data for figure 4.18.....	77
Table 4.9 Raw data for 2,6 DMN/2,7DMN ratio for the three sets of duplicate experiments.....	79

Table 4.10 Raw data for 2,6 DMN/2,7DMN ratio for the three sets of duplicate experiments.....	79
---	----

ACKNOWLEDGEMENTS

I would like to start by thanking my advisor Dr. Chunshan Song for his full support and guidance during the course of my study at Pennsylvania State University. Also, I would like to express my gratitude towards my committee members: Dr. Sarma Pisupati and Dr. Andre Boehman for serving on my committee. Special thanks to Dr. Pisupati for helping me out with my funding during my first semester in Pennsylvania State University. My thanks to Dr. Xiaochun Xu, a former CFCP (Clean Fuels and Catalysis Program) group member for helping me out initially when, I started on my experiments. My special thanks to Dr. Shyamal Kumar Saha for his guidance and helpful discussions. I would also like to thank all the past and present CFCP group members for their help and support both academically and personally during the course of my M.S research. I would finally like to thank the Department of Energy for their financial assistance for carrying out this research work.

Many people supported me throughout my work and this thesis will not be complete without thanking them. My friends at the Energy Institute, in EME and other departments – Late, Dr. D. Clifford, Maria, Nari, Pradeep, Prabhat, Gagan, Dania, Meredith, Krishna, Manodeep, Ravindra, Srilatha and Samrudhdi. I would like to thank Magda Salama and Nichole Wonderling at the MRI (Materials Research Institute). I would also like to thank Ms. Shelu Garg, Ms S.Vedurti Dr. Monoj Kumar and Dr.J.K. Gupta of Indian Institute of Petroleum, Dehradun for their help with microcalorimetry. I want to thank my family for their constant encouragement. I would like to convey my special thanks to my friend Ramya for her continual support and encouragement during my stay at Pennsylvania

State University. Last, but not the least, my thanks to Tejaswi, my husband, for his encouragement and support. Finally, I would like to dedicate this thesis to my father Dr. G. Murali Dhar who inspired me to pursue my interests in chemical engineering and catalysis.

Chapter 1

Introduction

In the 21st century fossil fuels have become the primary sources for energy production as well as dominant feed stocks for the production of chemicals and synthetic organic materials. As the world petroleum reserves are dwindling, the possibilities of the use of coal as a future energy source as well as a synthetic organic materials feedstock are being explored. Coal produces up to 75% of carbon dioxide emissions per unit of energy produced when compared to other fossil fuels (Song and Schobert, 1993). One of the major advantages in selecting coal as a feed stock for organic materials and specialty chemicals is that, carbon dominates the compositions of coal on a weight basis. Most of this carbon in the composition is already in the form of aromatic structures. This makes coal an ideal starting material for the aromatic chemical industry unlike the petroleum based feed stocks where carbon is mostly in the form of aliphatic structures. Naphthalene and its derivatives are richer in the oils from some bituminous coals. These aromatic structures especially those of naphthalene based compounds can be used in the synthesis of some of the new generation high strength polymer materials such as polyethyl naphthalate (PEN) and liquid crystal polymers (LCP's).

The compound 2, 6 – dialkylnaphthalene (2, 6 - DAN) is one of the major desired feedstocks for the synthesis of advanced polyester materials such as polyethylene naphthalate (PEN), polybutylene naphthalate (PBN). The most common industrial route

for synthesizing these polymers is to first synthesize and isolate the 2, 6-DAN isomer. The only commercial process is that by the BP-Amoco company that uses a $\text{HF}_3\text{-BF}_3$ based catalyst. This process is energy intensive and also brings forth an additional problem of the catalyst disposal. An alternative to this problem may be the exploration of the possible use of zeolites in the alkylation of naphthalene or alkylnaphthalene. Obtaining the feedstocks for this route is not very difficult as a lot of the products from the coal derived fuel synthesis are rich in naphthalene and naphthalene based compounds. Thus this can also be a value addition to the refinery processes. An additional advantage is that zeolites are environmentally benign and easier to handle. One of the main challenges in this step is to selectively enhance the formation of the desired 2, 6 - DAN isomer to the 2, 7-DAN isomer as the separation of the two isomers is very difficult.

This work has been carried out as a part of the ongoing DOE refinery integration project at the Pennsylvania State University involving the production of advanced liquid fuels, including diesel, jet fuels, gasoline as well as organic chemical synthesis from the blends of all these coal and petroleum derived middle distillates. This project deals with the synthesis of novel environmentally benign catalysts for the development of specialty engineering polymers. The objective of this work is to study the application of zeolite catalysts for the methylation of 2 - methylnaphthalene. The main focus of this study is to improve the 2, 6 - DMN/2, 7 - DMN selectivity as it is not possible to separate the two isomers by the existing physical separation techniques. The effects of the variation of the catalytic properties on modification of the catalysts with isomorphic substitution of iron

were also studied. The most important part is to develop a suitable catalyst favoring the yield of the 2, 6 - DMN isomer used in the development of specialty polymers.

Chapter 2

Literature Review

2.1 Industrial Processes for 2, 6 - Dimethylnaphthalene

2, 6-dimethylnaphthalene (2, 6-DMN) is a precursor to a polyester which has enhanced properties. 2, 6-dimethylnaphthalene can be oxidized and esterified to give dimethyl 2, 6-naphthalenedicarboxylate (2, 6-NDC). This monomer undergoes polycondensation with ethylene glycol to give polyethylenenaphthalate (PEN). PEN's properties offer considerable improvement over those of polyethyleneterephthalate (PET). The initial efforts for the development of 2, 6-NDC was investigated by BP Amoco as early as 1973 by carrying out the oxidation of 2, 6-dimethylnaphthalene that was isolated from heavy ultraformer bottoms (Lillwitz, 2001). The process flow diagram for the development by the BP Amoco process is given in the Figure 2.1 below.

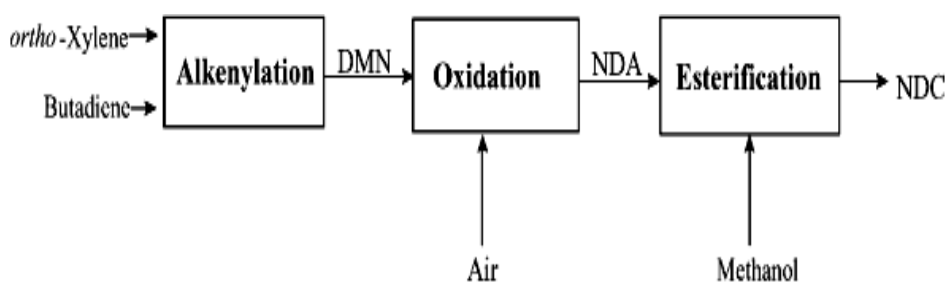


Figure 2.1 Flow diagram of BP Amoco 2, 6 - NDC process from Lillwitz 2001.

Some of the other companies that simultaneously investigated the production of 2, 6-NDA and subsequently worked on the development of 2, 6-dimethylnaphthalene are

Sun Oil and Teijin. They established a cooperative research program for the development of the best possible technologies for the manufacture of 2, 6-dimethylnaphthalene and the subsequent production of 2, 6-NDC and 2, 6-NDA. One of the routes were to isolate 2, 6-DMN obtained in the light cycle gas oil from the refinery streams by clathration of the DMN's with m-nitro benzoic acid but was later discarded because the dimethylnaphthalenes mixture isolated was insufficient to support the operation for one plant based on the forecasted demand. (Allen and Malmberg, 1966; Ogata and Shimosato, 1972). The other route they looked at was an o-xylene and butadiene based process but it did not materialize due to the insufficient market demand of the final polymer.(Eberhart et al., 1965 ; Harad et al., 1974).

Later on during the 1980's BP Amoco decided to adopt the above described Sun Oil and Teijin process for the development of 2, 6-DMN by the butadiene and orthoxylene condensation. In addition to the development of the butadiene and o-xylenes scheme, BP Amoco reviewed alternate technologies to produce 2, 6-NDA. One of the processes investigated was the 2-step carbonylation of naphthalene by the iodination of naphthalene by the Eastman Chemical Company. In the first step, the iodination of naphthalene was carried out to get 2, 6-diiodonaphthalene subsequently followed by carbonylation to directly produce 2, 6-NDA as shown in the following Figure 2.2.

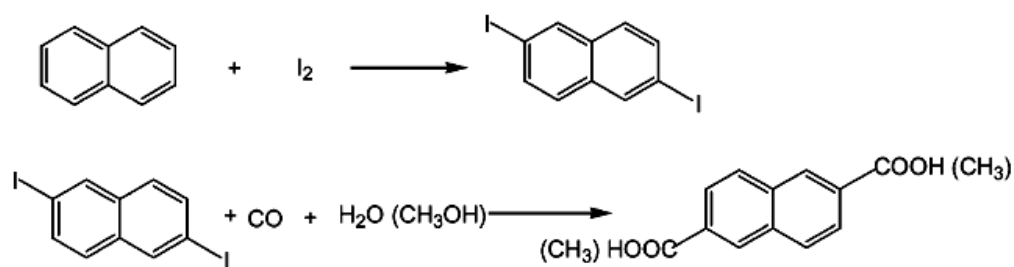


Figure 2.2 B.P Amoco's naphthalene carbonylation process from Lillwitz, 2001.

The catalysts used for oxidation were reported to be alkali and alkaline earth cations and basic faujasite zeolites (Tustin and Rule, 1994). Homogeneous rhodium and iodine were used as the catalysts for the iodination process (Steinmetz and Rule, 1989). This process failed to materialize due to the corrosive nature of iodine and also raised environmental concerns regarding the handling and disposal of the iodine systems. Additionally, the process had low conversions coupled with the difficulty of separating the iodo isomers. The second process reviewed for the production of 2, 6-DMN involved the carbonylation of toluene and butene. The carbonylation step of this process produces dialkylbenzene that is followed by hydrogenation, dehydration and dehydrocyclization to produce 2, 6-dimethylnaphthalene (Abe et al., 1991). The main plus point in this step is the elimination of the isomerization step as it selectively produces the 2, 6-DMN, the isomer of interest. The reaction is given in the Figure 2.3.

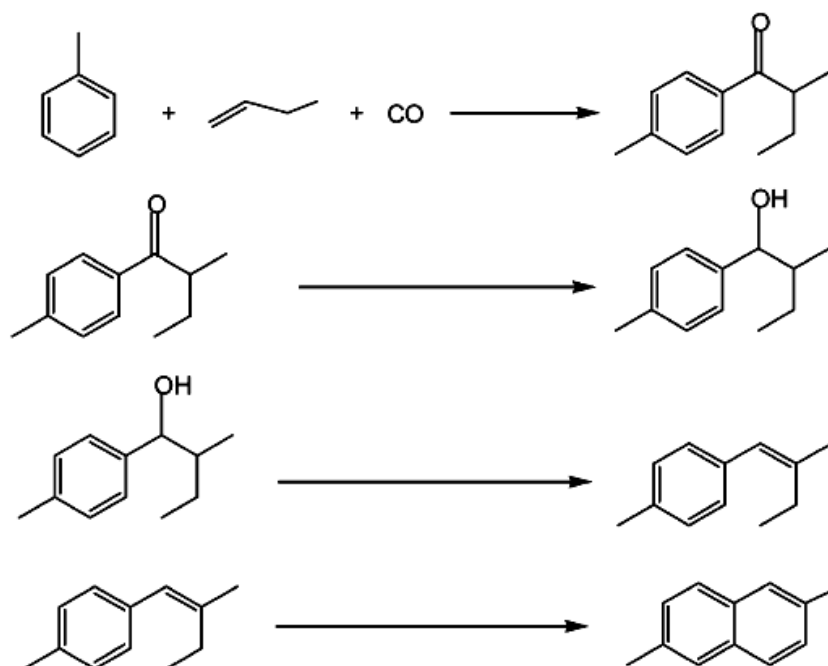


Figure 2.3 MGC carbonylation process from (Abe et al., 1991 and Lillwitz et al., 2001).

Another route competitive to this route was the carbonylation of *m*-xylene and propylene which is similar to the previously discussed iodination route except that the above process has a higher yield compared to the present process. This is because the dehydrocyclization reaction for this process is difficult and less selective. A major drawback for these carbonylation processes compared to the BP Amoco process is that the catalysts used for the above processes are fluoride based ($\text{HF}_3\text{-BF}_3$) and the handling and disposal of these catalysts causes an environmental concern (Abe et al., 1991). More recently in the 1990's several routes to the production of 2, 6-DMN was proposed based on the alkylation of naphthalene. A patent by Teijin (Sumitani and Shimada, 1992) describes a two step naphthalene alkylation process in which naphthalene is reacted with a DMN recycle stream to produce methylnaphthalenes which then undergo methylation

using methanol. Simultaneously, the DMNs are also isomerized in the presence of a zeolite based catalyst so that the ratio of 2, 6-DMN/2, 7-DMN is increased in the product. This chemistry has an edge over the other processes as it uses zeolites as catalysts for all the steps which are easier to handle compared to the traditional acid catalysts mentioned above. The yields of the desired compounds are very low and also a substantial amount of recycle is involved. Since 2, 6-DAN is the key precursor required in the development of 2, 6-NDC, more research is being carried out for the alkylation of naphthalene.

Mobil Technology Company and Kobe Steel developed a process based on the alkylation of naphthalene and then employing Kobe's separation technology using a large pore zeolite MCM-22 for both alkylation and separation processes (Angevine et al., 1991; Motoyuki et al., 1998). The source of these methylnaphthalenes was from the refinery isolated streams. A mixture of the two MN isomers was used as a feed for this process. Motoyuki et al., (1998) carried out the alkylation of the MN isomers and reported that the 2, 6-DMN /2, 7-DMN ratio dropped down to 1.2-1.5. The separation of these DMNs is not possible by the usual physical separation processes like distillation or crystallization as, the difference between the boiling points of the 2, 6-DMN isomer and the 2, 7-DMN isomer is 0.3°C , while during crystallization, they form eutectic crystals at a 2, 6-DMN / 2, 7-DMN ratio of 0.7. Thus, the main show stopper in choosing an efficient process is to find an efficient and economically viable process for producing the 2, 6-dimethylnaphthalene in high yields with the ratio of the 2, 6-DMN with the rest of the DMN isomers being very high compared to the equilibrium values.

2.2 Selective Production of 2, 6-DAN

The alkylation of naphthalene to dialkylnaphthalenes can lead to the formation of 10 possible isomers. The β, β selective alkylation of naphthalene over zeolite based catalysts can produce the dialkylnaphthalene isomers of 2, 3-DMN, 2, 6-DMN and 2, 7-DMN (Song, 2002).

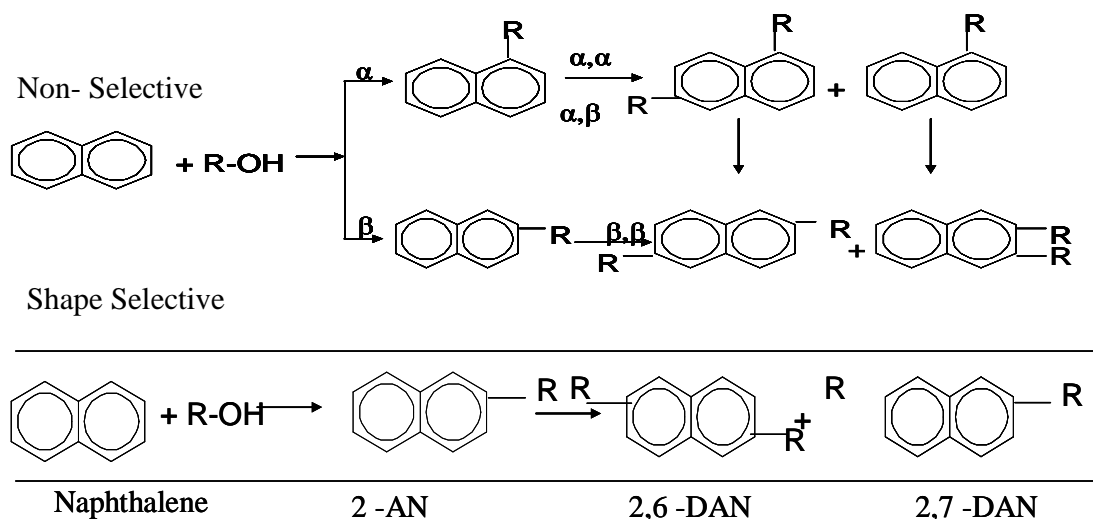


Figure 2.4 Schematic of naphthalene alkylation from Song, 2000.

The key challenge in this β, β selective alkylation is to obtain a high yield of 2, 6-DAN isomer especially by increasing the ratio of 2, 6-DAN to that of 2, 7-DAN. Since the source for the feedstocks is naphthalenes and alkylnaphthalenes, it was found that on fractional distillation of the methylnaphthalene streams based on their boiling points, the fraction taken out at 260°C to 265°C contained a majority of 2, 6-DMN and 2, 7-DMN. The fraction taken at 266°C to 270°C contained mostly 2, 3-DMN. Due to the close boiling points of the 2, 6-DMN and the isomers, it is very difficult to achieve 100%

separation of these isomers (Allen et al, 1966). It is more important to achieve a higher 2, 6-DMN to 2, 7-DMN ratio as it is very difficult to separate the both the isomers both form eutectic crystals at a ratio of 0.7. The higher theoretical weight percentage yield of dimethylnaphthalene (138%) for its oxidation to 2, 6-naphthalenedicarboxylate, gives it an edge over the other higher carbon chain substituted dimethylnaphthalenes (i.e. ethyl (117%) and isopropyl (102%)). This has led to a large focus in the 2, 6-DMN as the feedstock for the oxidation step in the processes for 2, 6-NDA/ 2, 6-NDC (Lillwitz, 2001). Though it is easier to selectively produce higher carbon number 2, 6-dialkylnaphthalenes, a lot of research has also been done in the selective production of 2, 6-diisopropylnaphthalene also.

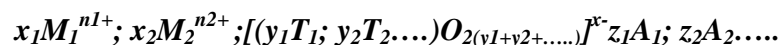
The alkylation of naphthalene on zeolite based catalysts has an edge over the synthetic o-xylene and butadiene route commercialized by BP-Amoco and the alkylation of benzene structures by Mobil as these routes involve steps for building the naphthalene structures. Thus it has been proposed that the routes based on alkylation of naphthalenes might have an economic advantage. Also the catalysts used in the above mentioned synthetic routes were either an $\text{HF}_3\text{-BF}_3$ based catalyst or AlCl_3 based catalysts as opposed to zeolites for the naphthalene alkylation processes. Some of the various zeolite based catalysts employed for the naphthalene alkylation processes developed are ZSM-5 (MFI), ZSM-11 (MFI/MEL), ZSM-12 (MTW), mordenite (MOR), Y (FAU), FAU/EMT, Beta, MCM-22 (MWW), and NU-87 (NES) (Millini et al., 2003). The most common zeolites used for naphthalene alkylation reported were mainly medium pore zeolites

(ZSM-5, MFI type) where as the isopropylation of naphthalene involved large pore zeolites (MOR, Y, BEA, ZSM-11).

2.2.1 Zeolites

Zeolites are a group of hydrated, microporous, crystalline aluminosilicates containing exchangeable cations of group IA and IIA elements (i.e. Na^+ , K^+ , Mg^{2+} and Ca^{2+}), which reversibly adsorb and desorb water. They were discovered by a Swedish mineralogist Cronstedt, in the year 1756, who derived the name “zeolite” from the two Greek words for “boiling stone” (Zein and Lithos) (Tomlinson, 1998). Weitkamp and Puppe (1999) defined zeolites as crystallized solids characterized by a structure consisting of a three dimensional and rectangular framework formed by linked TO_4 tetrahedra where (T = Si, Al), each oxygen being shared between two T elements. They contain channels and cavities with molecular sizes that can host charge compensating cations, water, other molecules and salts. The microporosity must be open and the framework must have enough stability to allow the transfer of matter between the interior of crystals and the exterior.

The generic composition of a zeolite is best described by the general formula:



In the above formula, the expression in square brackets represents the framework composition of the zeolite (Song, 2002). The other terms in the formula are

- M_1 and M_2 cations with charge n_1, n_2 which compensate the negative charge of the framework ($x_1n_1 + x_2n_2 + x_3n_3 + \dots = x$)
- T_1, T_2 etc are elements (Si, Al.....) in the tetrahedral
- A_1, A_2 , are water, molecules or ion pairs.

Zeolites have found wide considerable use as environmentally benign catalysts due to several preferable properties. They have a well-defined crystal structure, high internal surface area, a definitive pore structure, good thermal stability and the ability to adsorb and concentrate hydrocarbons. Si is the principal element in the framework, and when replaced by Al, a negative charge is generated in the framework. This negative charge is balanced by cations of group IA and IIA elements, which can be ion-exchanged with H^+ to form an acidic support.

The acidic properties of zeolites are very important for their application as catalysts. The acidity of a zeolite is defined by three parameters: *acid strength, acid-site density and acid – site type*. There are two types of acid sites, examples of which are depicted in the following Figure 2.5. The Brønsted acid sites are proton donors and Lewis acid sites are electron pair acceptor.

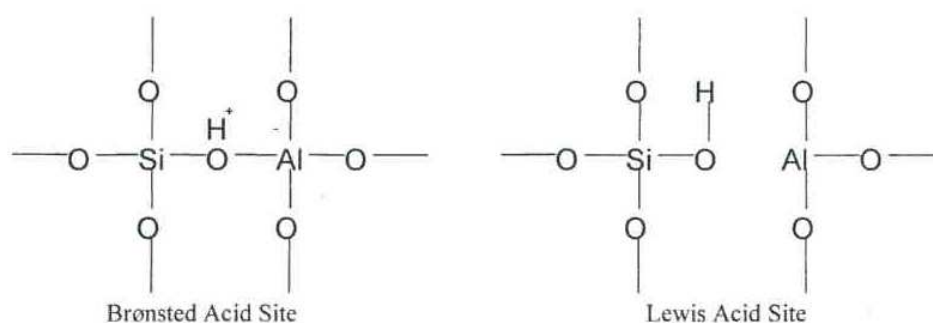


Figure 2.5 Examples of bronsted acid and lewis acid sites in the zeolite framework

The temperature programmed desorption (TPD) using basic probe molecules is a common method for characterizing the type of acid sites in zeolites (Turaga et al., 2000). Infrared Spectroscopy of adsorbed pyridine is also a well-established technique to investigate acid types in zeolites. Pyridine sorbed onto zeolite structures gives very sharp bands which selectively indicate the presence of Brønsted acid sites, Lewis acid sites and cations. Generally the majority of the acid sites in a zeolite are Brønsted acid sites but if the zeolite is calcined at high temperatures, they form Lewis acid sites (Ward, 1967). In general, the zeolite acidity can be correlated with $\text{SiO}_2/\text{Al}_2\text{O}_3$ mole ratio (Eberly Jr. et al., 1971; Beaumont and Barthomeuf, 1972). Zeolites with a lower $\text{SiO}_2/\text{Al}_2\text{O}_3$ ratio will have a higher acidity.

2.2.2 Shape Selectivity in Zeolites

The shape selectivity in zeolites can be defined by the molecular-sieving function in action during a catalytic reaction which distinguishes between the reactant, the product or the transition state of the reacting species based on the relative sizes of the molecules

and the pore spaces where the reactions occur. (Song et al., 2000) The shape selectivity can be classified into three main types as discussed below.

The selective conversion of certain reactant molecules in comparison to other types of molecules in the feed stock of reactants based on the molecular size of the reactant in question with respect to the pore size of the zeolite is known as reactant shape selectivity. The intra pore diffusional characteristics of the reacting molecules govern this type of selectivity (Song et al., 2000). One of the common examples of reactant shape selectivity is the selective dehydration of n-butanol and iso-butanol over CaA from a mixture of n-butanol and iso-butanol in the Figure 2.6 (Song et al., 2000).

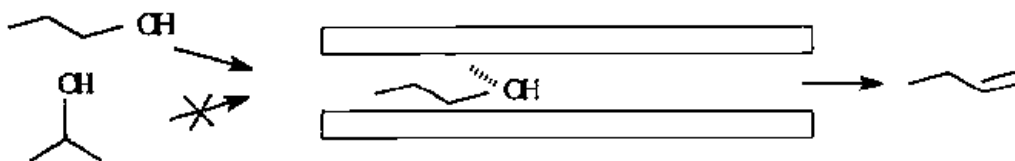


Figure 2.6 Reactant shape selectivity in alcohol dehydration reactions (Song et al., 2000).

The selective formation of certain products of a reaction over the other thermodynamically favored products owing to the smaller size of the desired product permits easy diffusion out of the pore channel, while the diffusion of other bulkier products is limited by the relatively smaller pore size of the zeolite catalyst is product shape selectivity. Similar to the reactant selectivity, the product selectivity is also dependant of the inter pore diffusion characteristics of the molecules in question. The methylation of toluene and isomerization of xylenes on ZSM-5 catalysts perfectly

advocates product selectivity. Though the p-xylene isomer is not the thermodynamically preferred product, the diffusivity of the para isomer is higher by an order of magnitude than that of the ortho and meta xylene isomers (Song, 2000).

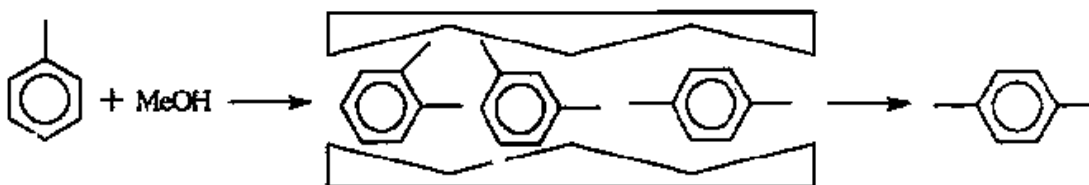


Figure 2.7 *Product Shape Selectivity in the methylation of toluene (Song, 2000.)*

Transition state selectivity occurs when certain steric restrictions are imposed by the pore channel geometry near the active sites on the transition state of the reacting molecule. This state does not depend on the crystal size or the activity of a zeolite but depends on the pore geometry and zeolite structure. A good example of the transition state selectivity is the acid catalyzed disproportionation of dialkylbenzenes over H- Mordenite. Typically the acid catalyzed disproportionation of dialkylbenzenes is carried out on silica-alumina or large pore zeolites like HY. At equilibrium conditions, the primary product obtained is 1, 3, 5-trialkylbenzene, however when the reaction is being carried out using H-Mordenite as a catalyst, the diphenylmethane like transition state leading to the formation of 1, 3,5-trialkyl benzene-isomer does not fit within the 12 – ring channels of H Mordenite.(Song et al., 2000).

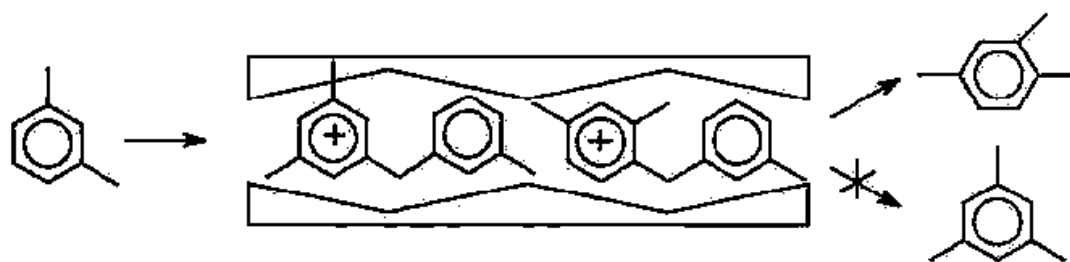


Figure 2.8 Transition shape selectivity in *m*-xylene disproportionation reaction (Song *et al.*, 2000).

There is a fourth kind of shape selectivity proposed by Song *et al.* (1999) called the restricted electronic transition state selectivity. It is a new concept that states that the higher frontier electron density of the isomer positions of a molecule can promote the formation of the isomer at that particular position even when the other isomeric positions are electronically favored. A good example of the restricted electronic transition state selectivity is the preferential formation of the 2, 6-diisopropylnaphthalene (2, 6-DIPN) during the alkylation of 2-IPN over H-Mordenite. It has been reported by Song *et al.* (1999) that the frontier electron density (f_rE) for the electrophilic substitution over the position 6 is higher than that of the position 7 of the 2-IPN molecule during the isopropylation of 2 Isopropyl Naphthalene (2-IPN). In this work, H-ZSM-5 and H-Mordenite and H-Y Zeolite were chosen as the main catalysts for the methylation of 2-methylnaphthalene based on the literature. MFI type zeolites were found to be ideal for the methylation of naphthalene while mordenite has been identified as an ideal catalyst for the isopropylation of naphthalene.

2.2.2.1 Y Zeolite

Zeolite Y, A faujasite type zeolite is one of the widely used, large pore zeolite. It possesses a three dimensional network of interconnecting channels. The pore diameter is identical in each of the x, y, z coordinate. The main cavities in the zeolite Y are 11.2 Å in diameter and are interconnected through 12 membered ring pore openings 7.4 Å in diameter (Baerlocher et al., 2001). The following Figure 2.10 depicts the structure of the zeolite Y.

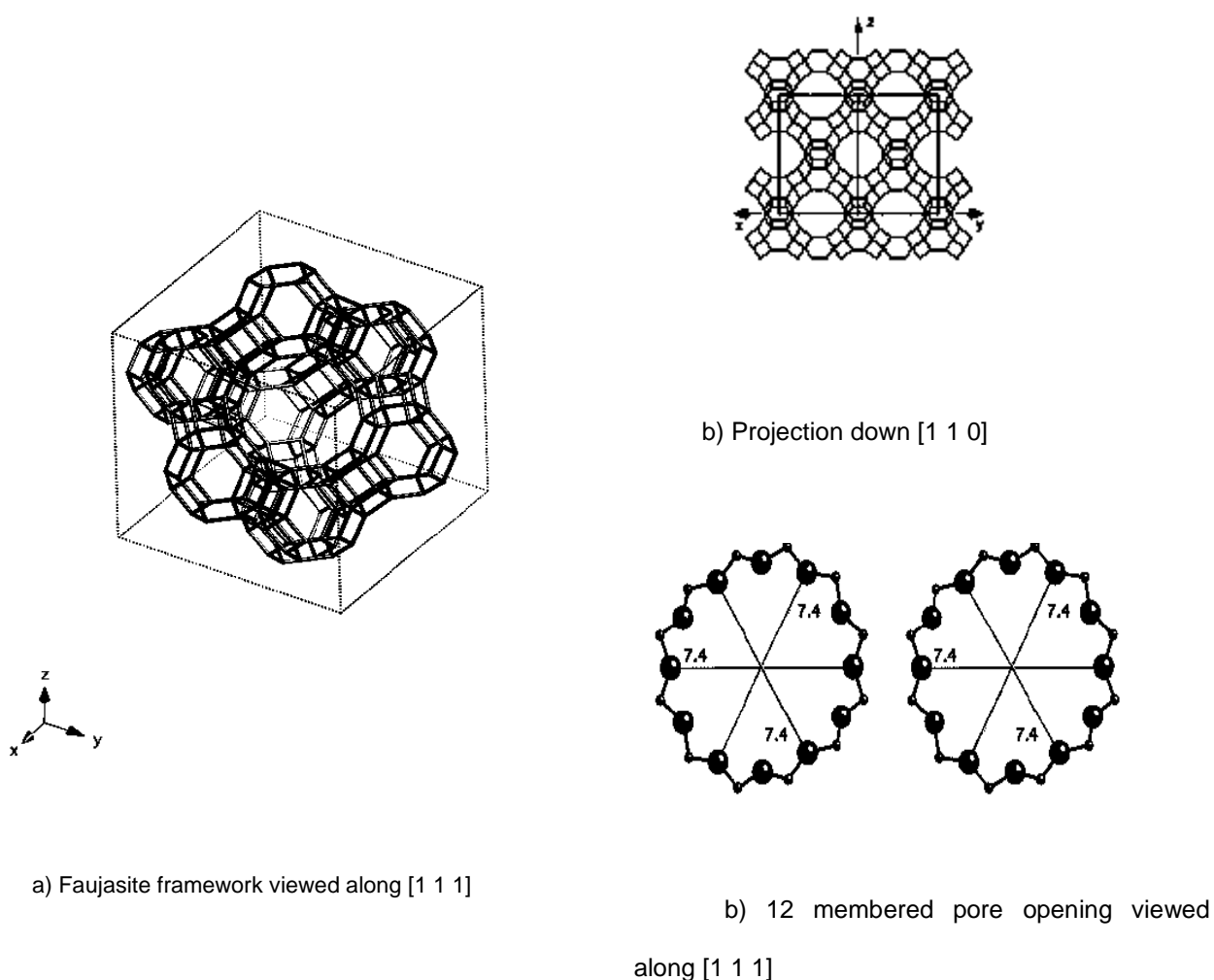


Figure 2.9 Crystalline structure of Y zeolite (Dimensions in Å) (Baerlocher et al., 2001)

2.2.2.2 Mordenite

The structure of mordenite zeolite is shown in the following Figure 2.10. Mordenite has a channel like pore structure with side pockets. The main channels are 6.5 Å by 7.0 Å. The side pockets measure 5.7 Å by 2.6 Å (Baerlocher et al., 2001).

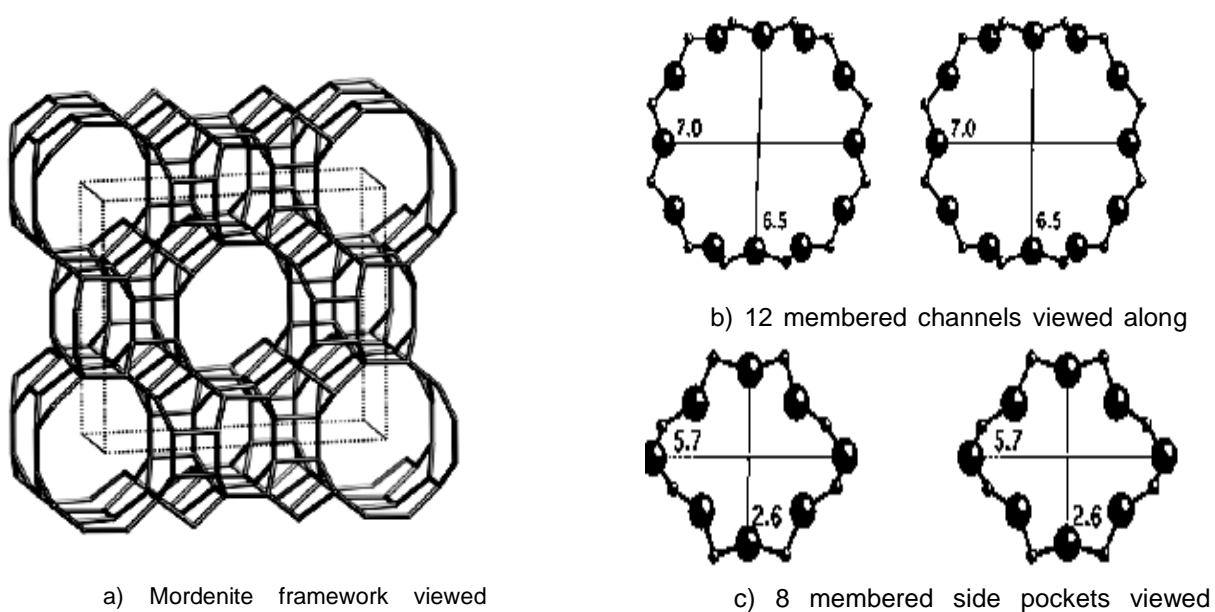


Figure 2.10 Crystalline structure of Mordenite (Dimensions in Å) (Baerlocher C. et al., 2001.)

2.2.2.3 ZSM-5

ZSM-5 has an interesting two dimensional pore structure. Both the channels are from 10 membered oxygen rings. One set of pores is straight and elliptical in cross section with dimensions of 5.5Å by 5.1Å. The other set of pores is circular, and intersects

the straight pores at right angles, in a zigzag pattern. The dimensions of these pores are 5.6 Å by 5.3 Å. The following Figure 2.12 shows the ZSM-5 zeolite structure.

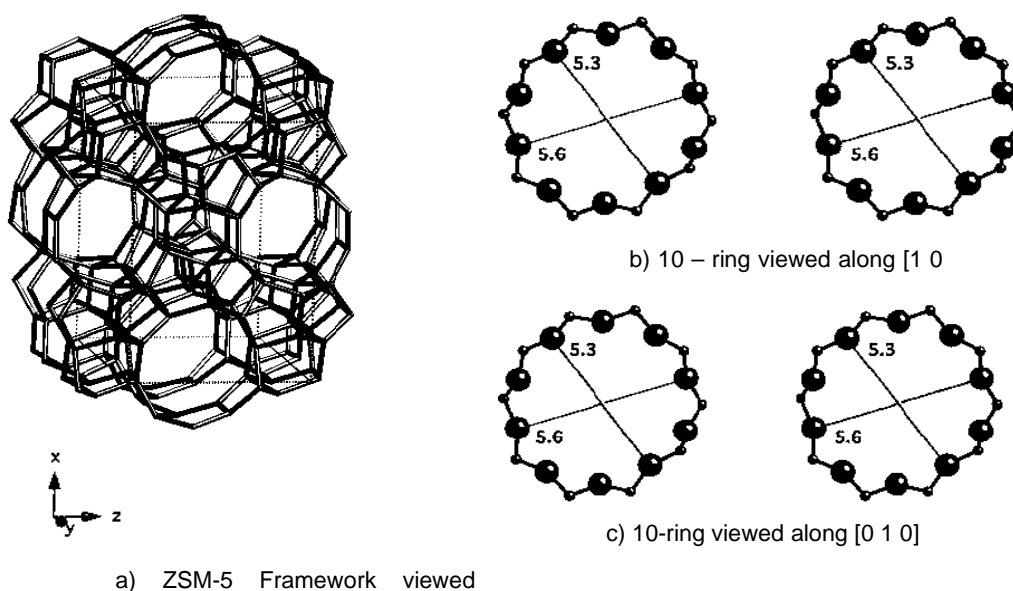


Figure 2.11 Crystalline structure of ZSM -5 (Dimensions in Å) (Baerlocher et al., 2001).

2.3 Alkylation of Naphthalene

Song et al. (2002) described that the shape selective alkylation of naphthalene can produce 2, 6-DAN, the molecule of interest for producing various specialty polymers as discussed in the sections above. The β , β selective alkylation of naphthalene can produce 2-alkylnaphthalene, 2, 3-DAN, 2, 6-DAN and 2, 7-DAN. The key challenge is to isolate the 2, 6-DAN with a high selectivity. The following Figure 2.13 shows the non selective and shape selective alkylation routes for the alkylation of naphthalene.

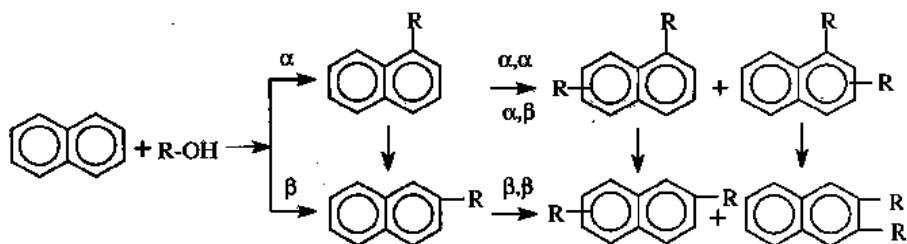


Figure 2.12 Schematic of alkylation of naphthalene from Song, 2000.

2.3.1 Isopropylation of Naphthalene

The isopropylation of naphthalene over mordenite and Y zeolite carried out at 240°C in a batch autoclave reactor for 5h using propene or propan-2-ol as the alkylating agent yielded the preferential formation of 2, 6-diisopropylnaphthalene (2, 6-DIPN) at a 2, 6-DIPN/2, 7-DIPN ratio of ~2 on H Mordenite and a ratio of about 1 on H Y as the catalyst. (Katayama et al.; 1991). Moreau and coworkers carried out isopropylation of naphthalene and 2-Isopropylnaphthalene on H-Mordenite and Y Zeolite using isopropyl bromide as alkylating agent (Moreau et al., 1992) The results showed that the 2, 6- and 2, 7-disubstituted products were formed in equal yields with a ratio of around 1 when using unmodified H-M and Y-zeolite catalysts. However, when the isopropylation was carried out on Y zeolites modified by the silanation method to neutralize the external surface sites, they reported an overall increase in the β Selectivity though the 2, 6-DIPN /2, 7-DIPN ratio was the same as that for the unmodified catalysts. Song (2000) reported the isopropylation of naphthalene in presence of mesitylene (1, 3, 5 – TMB) as a solvent and achieved a 2, 6-DIPN selectivity of 67% on mordenite as opposed to 16% on Y zeolite. Song and Kirby (1994) reported over 65% 2, 6-DIPN selectivity and 2, 6-

DIPN/2, 7-DIPN ratio about 3 by carrying out the isopropylation of 2-isopropylnaphthalene using Isopropanol as the alkylating agent on partially dealuminated mordenite catalysts. Schmitz and Song (1996) reported a 2, 6-DIPN/2, 7-DIPN ratio > 2 using propylene as the alkylating agent on partially dealuminated mordenite. They concluded that partially dealuminated proton-form mordenites exhibit more shape-selective properties during the isopropylation of naphthalene when compared to the parent unmodified mordenites.

Moreau et al. (1996) carried out the liquid phase alkylation of naphthalene using hindered alkylating agents like cyclohexyl derivatives, cyclohexylbromide or cyclohexene over efficiently over HY zeolites at 200°C. They reported both high conversions and convenient β,β selectivities at very short reaction times. Though the 2, 6- / 2, 7-dicyclohexylnaphthalene ratio was reported to be 1 similar to the isopropylation reported in an earlier paper (Moreau et al.,1992), the yield of trialkylnaphthalenes was found to be considerably lower and the resulting 2, 6-dicyclohexylnaphthalene, a crystalline compound that can be easily separated from the reaction mixture by crystallization. It has been indicated that the molecular size of 2, 6-DIPN is slightly smaller than 2, 7-DIPN isomer (Song and Kirby,1994). The computer simulation studies done by Horsley et al.(1994) indicate that the diffusion of 2, 6-DIPN inside the mordenite pore channel is easier than that of 2, 7-DIPN. This partially supports the observed selectivity of mordenite for 2, 6-DIPN and a higher 2, 6-DIPN/2, 7-DIPN ratio. Song et al. (1999) calculated the critical diameters for 2, 6-DIPN and 2, 7-DIPN using MOPAC and reported that 2, 6-DIPN (7.21Å) has a slightly smaller critical diameter

compared to that of 2, 7-DIPN (7.26Å). Schmitz and Song (1996) reported improved 2, 6-DIPN/2, 7-DIPN ratios by using water and dealuminated mordenite for enhancing the shape selectivity of the catalyst. Kim et al. (1995) reported that there was a more selective 2, 6-DIPN formation inside the pores as opposed to the non selective reactions that led to the subsequent coke formation on the external surface of the catalyst. The same group (Kim et al., 1995) reported upto 70% 2, 6 - DIPN selectivity in an isopropylation reaction on ceria impregnated H Mordenite catalysts. Schmitz and Song (1996) reported that the higher selectivity towards 2, 6 - DIPN on partially dealuminated mordenite might be due to the lower reactivity of the dealuminated mordenite catalyst. This concurs with the above reported results by Kim et al. (1995) that the external non selective reactions have a low 2, 6-DIPN selectivity. Thus by inhibiting the surface reactions by partial dealumination of mordenite, we have inhibited the occurrence of the external non selective reactions thus increasing the dialkylnaphthalene selectivity but this reports the overall conversions of the reactions compared to those carried out on the parent catalysts.

2.3.2 Methylation of Methylnaphthalene

The selective synthesis of 2, 6-dialkylnaphthalenes has focused on solid acid catalysts providing shape selectivity. The methylation of naphthalene yields 10 disubstituted isomers including α , α (1, 8-DMN, 1, 4-DMN, 1, 5-DMN) α , β (1, 2-DMN, 1, 3-DMN, 1, 6-DMN, 1, 7-DMN) and β , β (2, 6-DMN, 2, 7-DMN, 2, 3-DMN) isomers. The key challenge is to isolate the 2, 6-DMN isomer during the β alkylation. It is difficult to observe a shape selective effect during the methylation of methyl naphthalene

as opposed to the isopropylation of naphthalene as the molecular size difference between the 2, 6-DMN and 2, 7-DMN isomer is very small (Tanabe and Holderich, 1999). The first efforts in the shape selective methylation of naphthalene and methylnaphthalene were reported in literature by Fraenkel et.al. (1986). They carried out methylation of naphthalene using methanol as the alkylating agent on a tubular flow reactor and temperatures between 300°C to 500 °C on H-mordenite, H-Y and HZSM-5. It was reported that β selective alkylation was favored both for naphthalene and 2-MN on HZSM-5 but the conversion was very low. Though H-Y and H-M exhibited higher conversion, they had low β selectivity. It was reported that the ZSM-5 type catalysts favored the β position and the naphthalene is most probably methylated at its β position in the so called half cavities in the zeolite. Neuber and Weitkamp (1991) reported that the observed product shape-selectivity effects could be due to the diffusional restrictions for the reactant and product molecules inside the pores of zeolite HZSM-5 as opposed to the half cavities on the surface of the catalyst as proposed by Fraenkel et al. (1986); Klein et al. (1994) also reported that the 2-methylnaphthalene alkylation takes place inside the pores of HZSM-5 and the most probable sites of the reaction would be at the intersection of the sinusoidal and straight channels based on molecular mechanics calculations supported by powder X-Ray diffraction analysis. They further mentioned that the alkylation at the half cavities occurred in addition to the methylation inside the pores.

Komatsu et al. (1994) carried out the methylation of methyl naphthalene on MFI-type catalysts reported that the poisoning of the external surface active sites by 2, 4-dimethylquinoline improved the selectivity of the reaction towards 2, 6-DMN as the

neutralization of the surface sites prevented the surface isomerizations and the non selective reactions yielding undesired isomers. Inui et al., (1996) carried out the methylation reaction with a mixture of α and β methylnaphthalenes and methanol on a ZSM-5 catalyst at 400°C. The catalyst surface was neutralized using BaO. Though the initial activities were lower than that of the parent ZSM-5 zeolite, the β , β selectivities was reported to higher than that compared to the ZSM-5 but the conversion was very low. Also, the catalyst life was enhanced by the neutralization. Pu et al., (1996) reported improved selectivity towards the 2, 6-DMN on the use of transition metal modified MFI-type catalysts as well as large pore zeolites like BEA and Y Zeolites using β -methylnaphthalene as feed with 1-Methylnaphthalene, tetralin and mesitylene as solvents. The experimental conditions were same as that were reported by the above paper (Inui et al., 1996).

The increase in the 2, 6-DMN selectivity on the transition metal modified catalyst is because the modification decreases the acidity thus reducing the possibility of further isomerization of 2, 6-DMN to 1, 6-DMN which is aided by strong acidity. They concluded that the higher selectivity towards the β alkylation was due to the lower acidity as proposed in literature (Komatsu et al., 1994). In the large pore zeolites, the zeolite BEA exhibited the highest selectivity and activity towards the formation of 2, 6-DMN due to the 3 – dimensional 12 membered oxygen rings without the super cage. The ZSM-5 was isomorphously substituted using the transition metals and the substitution was confirmed by the absence of an additional metal oxide peak and the similar XRD patterns of the modified samples to that of the parent catalyst samples (Inui et al., 1993). It was

reported that the activity of the MFI-type catalysts was lower than that of the parent HZSM-5 as the acidity was significantly lowered confirmed by the NH_3 -TPD by a shift of the peak towards the lower temperature region confirming that the acidity has been lowered. The use of tetralin as a solvent for the reaction reported very low coke formation on BEA compared to mesitylene as it stabilized the catalyst preventing rapid deactivation.

Komatsu et al., (2000) recently reported on the selective formation of 2, 6-dimethylnaphthalene (2, 6-DMN) from methylation of 2-methylnaphthalene with methanol on HZSM-5 and metasilicates with MFI- type structure. Their methylation results demonstrated that the isomorphous substitution of Al by other elements, such as B and Fe, or the deactivation of external surface (by using basic nitrogen compounds) can increase the selectivity to 2, 6-DMN. They reported a 2, 6-DMN/2, 7-DMN ratio of about 1.8 on Fe-MFI catalysts compared to a 2, 6-DMN/2, 7-DMN ratio on HZSM-5. The poisoning of the external surface by 2, 6-DMQ on the both the modified catalysts and the parent catalysts reduced the other isomer yields thus increasing the 2, 6-DMN yield. They concluded that in order to obtain 2, 6-DMN in high selectivity, it is effective to weaken the acid strength while keeping the pore dimension of MFI structure constant (or wider, if possible), which can be achieved by using Fe-MFI as a catalyst. Song et al., (2005) patented the process for isomorphous substitution of Al with transition metals into HZSM-5. They reported a high 2, 6-DMN/2, 7-DMN ratio of 1.8 -2.2 in the yield of the methylation of 2 - MN on Fe – modified catalysts.

Jin et al., (2006) studied the methylation reaction on microcrystalline ZSM-5 substituted by Zr and Si for Al in the framework at 400°C with a feed ratio of 1:5:3 2-MN; methanol and mesitylene. The products of the reaction were analyzed by gas chromatography. They reported a very high 2, 6-DMN/2, 7-DMN ratio of about 3.0 but a very low 2-MN conversion and catalyst life. While the incorporation of Zr in the zeolite framework reduces the acidity, the incorporation of Si increases the stability of the catalyst while reporting a ratio of 2, 6-DMN/2, 7-DMN of about 2. The acidity changes were characterized by NH₃-TPD and the structural changes were characterized by XRD, framework IR. As the dealumination increased, the crystallinity slightly increased and the slight shift of the peak from about 1100cm⁻¹ to 1097cm⁻¹ caused by a linear increase in the TOT vibrations with increasing metal concentration in the zeolite framework.

2.3.3 Proposed Reaction Pathways for the Shape Selective Formation of 2, 6-DMN

Several reaction pathways were proposed for the methylation of 2-MN based on both experimental and modeling studies. Fraenkel et al., (1986) proposed that the sites for the β -selective methylation of naphthalene were not in the pores of the ZSM-5 zeolite but in the half cavities on the external surface of the zeolite. Neuber and Weitkamp (1991) reported that the observed shape-selectivity effects could be due to the diffusional restrictions for the reactant and product molecules inside the pores of zeolite HZSM-5. Komatsu et al., (2000) carried out methylation of methylnaphthalene on both the protonated form of ZSM-5 and also on modified MFI-type zeolites. They compared their

results to their previous works reporting the poisoning of the external sites using 2, 4-DMQ (Komatsu et al., 1994). Based on these results, they suggested reaction pathways for the methylation of 2-MN both on the surface and the pore. The following Figure 2.13 depicts the reaction pathways during the methylation of 2-MN.

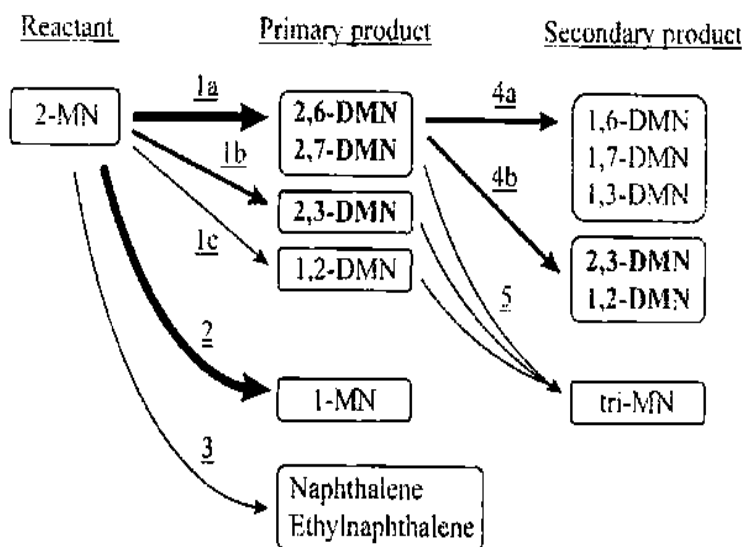


Figure 2.13 Reaction Pathways for methylation of 2 - methylnaphthalene from (Komatsu et al., 2000.)

It was proposed that during the initial stages of the methylation of 2-methylnaphthalene, the β selective methylation is carried out in the pore to give out primarily 2, 6-DMN and 2, 7-DMN and minor quantities of 2, 3-DMN. The initial reactions occurring simultaneously on the surface lead 1, 2-DMN and isomerization of 2-MN to 1-MN. Some residual amount of naphthalene and ethylnaphthalenes were formed. These above mentioned products sometimes react to form the secondary products like 1,

6-DMN, 1, 7-DMN and 1, 3-DMN through secondary isomerization on the external surface. It has further been reported that very minimal isomerization occurs in the pore from 2, 6-DMN and 2, 7-DMN to 2, 3-DMN and 1, 2-DMN occurs. Thus it can be said that the poisoning of the external surface sites helps in the retardation of these secondary reactions. It has also been reported that the narrower pore dimensions promote the 2, 7-DMN formation. Hence it is important to selectively reduce the surface acidity of the catalyst while trying to maintain the pore diameter constant or slightly larger. The molecular orbital theory reported by Song et al., (1999) reported that the higher electron density of the highest occupied molecular orbital (HOMO) at the C – 6 position in 2-MN compared to that at the C – 7 position prefers the formation of 2, 6-DMN electronically to the formation of 2, 7-DMN. Millini et al., (2003) carried out modeling studies on the alkylation of naphthalenes and methylnaphthalenes as well as the isomerization of the other DMN isomers to 2, 6-DMN. The diffusion pathways of the 2-methylnaphthalene in various large pore and medium pore zeolites were calculated. The results revealed that the diffusion of 2-MN in medium pore zeolites is predicted to be difficult compared to its diffusion in large pore zeolites. The pore intersections for the MFI-type zeolites allow the diffusion of the two isomers. Though the selectivity of the MFI-type zeolites towards the 2, 6-DMN is higher, the activity of the catalyst is very low. The formation of 2, 6-DMN and 2, 7-DMN is governed by the transition state selectivity. Fang et al., (2006) carried out computational analysis of the molecular dimensions of the dimethylnaphthalene (DMN) isomers and the reactivity difference of different carbon atoms in 2-methylnaphthalene (2-MN) by using the density functional theory. They reported that 2, 7-DMN is slightly smaller than 2, 6-DMN in molecular dimension which is why the 2, 6-

DMN/2, 7-DMN ratio decreases when the pore size of ZSM-5 narrowed. Similar to the results shown by Song et al., (2000), the calculations show that the position 6 in 2-MN is more reactive than position 7, which suggests that formation of 2, 6-DMN is electronically more favored than that of 2, 7-DMN inspite of the 2, 7 DMN isomer is relatively the same size.

2.4. Catalyst Modification Processes

Modification of zeolite catalysts may be done by either selectively neutralizing the external surface sites or by isomorphous substitution of transition metals into the zeolite framework.

2.4.1 External Surface Neutralization

The selective neutralization of external surface sites of ZSM-5 can be carried out by various techniques like ion exchange, poisoning with 2, 4-dimethylquinoline, chemical vapor deposition, dealumination, mechanochemical methods by mixing with, metal oxides like MgO, BaO etc, impregnation with phosphorous etc.

In ion exchange, the samples are exchanged with solutions of ammonium halides and the appropriate alkali cations in their nitrate forms to replace the some of the Al ions in the zeolite framework. (Vinek et al., 1991). The poisoning of the external surface sites with 2, 4 - dimethylquinoline was reported by Komatsu et al, (1994). They suggested the poisoning of the external surface sites for reducing the competitive reactions on the surface of the zeolite in an attempt to increase the 2, 6-DMN selectivity in the

methylation of methyl naphthalene reaction. HZSM-5 zeolites have been modified by chemical vapor deposition of silicon alkoxide to aid in improving the selectivity of the *p*-isomer in toluene disproportionation reaction (Hibino et al., 1991). It was reported that the modification of the ZSM-5 resulted in the narrowing of the pore-opening size and the inactivation of the external surface. Subsequently, the high selectivity of the *p*-isomer was caused primarily by the narrowing of the pore-opening size. Inui et al., (1996) reported improved 2, 6-DMN selectivities by employing BaO modified ZSM-5 as catalysts. The modification was done by a mechano-chemical method where the proton form of the zeolite was milled with barium acetate supported on fine silica particles in an agate mortar and subsequent calcining in air. TPD was used to characterize the acidity properties and it was concluded that this method enabled only in neutralizing the external surface of the sample. While the above processes effectively neutralize the surface acid sites, they have disadvantages like the pore size reduction and/or subsequent blocking of pore openings and channels. Excessive dealumination might also cause the collapse of the structure of the catalyst.

2.4.2 Modification by Isomorphous Substitution in the Zeolite

The incorporation of the transition metals in the framework of the zeolite can be either done during the hydrothermal synthesis of the zeolite or by post modification procedures. Pu et al., (1996); Komatsu et al., (1994) and Xu. et al., (1999) reported improved 2, 6-DMN selectivity by employing catalysts modified by direct hydrothermal synthesis by planting the desired atom in the original synthesis method. Song et al., (2005) patented a process for the post treatment of parent catalysts with corresponding

metal fluorides where in the resulting catalyst undergoes partial dealumination and has both Fe and a significant portion of aluminum present in the sample. In this method, the catalyst is slurried with a soluble metal fluoride salt. The incorporation of Fe in the zeolite framework might bring about a pore expansion by introducing a Fe – O bond (1.84 Å) causing a modification of the catalysts selective behavior.

2.5 Application of Literature Concepts to the Hypothesis

It is evident from the literature cited that the methylation of methylnaphthalene is predominantly influenced by the catalyst properties such as the catalyst structure, acidity and the pore size. It is hypothesized that the use of zeolites like ZSM-5 as catalysts for methylation of naphthalene may support the β -alkylation and aid in the selective formation of 2, 6-DMN. The isomorphous substitution of metals like Fe, Ti, Zr into the zeolite framework may lower the overall acidity of the catalyst and improve the selectivity of 2,6-DMN/2,7-DMN during the methylation of methylnaphthalene.

In this work, different types of zeolites will be tested to determine the effects of the zeolite pore structure, acidity on the methylation of 2-methylnaphthalene. The effects of the temperature of the reaction to the desired compound selectivity will also be examined. The medium pore zeolite ZSM-5 is modified by the isomorphous substitution of Fe into the framework of the zeolite since it has been shown in literature that the modification of the zeolite with Fe aids in the selectivity of the reaction. The modification of Fe will be carried out for six different Fe concentrations and the effect of the acidity changes will be quantified by the different acidity characterization techniques.

It is hypothesized that, in general, catalysts with moderate acidity promote the β selectivity of the reaction. For the same reason, it is believed that the modification of the catalyst with Fe using the isomorphous substitution improves the 2, 6-DMN yield and selectivity. It might also be possible that during modification, there might be a slight alteration in the pore dimensions of the zeolite thus influencing the shape selective properties of the catalyst. The effect of the iron content of the zeolite on the 2-methylnaphthalene reaction will also be studied. Several characterization studies have been carried out on the modified zeolite samples to determine the structural changes in the zeolites before and after the isomorphous substitution of Fe in the framework of the zeolite.

Chapter 3

Experimental

3.1 Catalyst Preparation

The different zeolites used as catalysts in this study are listed in the Table 3.1. All the zeolites used were received from Zeolyst International (Formerly PQ Corporation). All the zeolite supports were first calcined in airflow (~60mL/min) at 550°C for 5 hours at a heating rate of 1.8° C/min, before catalyst preparation. Thus, the zeolites that were received in the NH₄⁺ form were converted to the H⁺ form. The properties of the zeolites used in this work are listed in the Table below in their as received state.

Table3.1: *Properties of the zeolites, as Received*

Zeolite Type	Manufacturer	Zeolite Code	SiO₂/Al₂O₃ Ratio	Surface Area (m²/g)	Cation Form
Mordenite	Zeolyst	CBV 90A	90	500	H ⁺
Y Zeolite	Zeolyst	CBV 780	80	780	H ⁺
ZSM - 5	Zeolyst	CBV 8014	80	425	NH ₄ ⁺
ZSM - 5	Zeolyst	CBV 5524G	50	425	NH ₄ ⁺

The CBV 5524G catalyst was calcined in air as mentioned above and converted into the H⁺ form. This catalyst was used as the parent zeolite for all the samples modified by isomorphous substitution. The modification method followed was done following the wet chemistry method patented by Song et al., (1999). About 15g of the parent zeolite was used for each modification. For each sample, about 15g of H ZSM -5 is mixed with 150 g of distilled water. This zeolite water slurry is heated in an oil bath maintained at 92°C ± 5°C while stirring it continuously for 1 hour using a magnetic stirrer and a reflux column. Varied ratios of FeF₃.3H₂O and NH₄HF₂ were dissolved in 100g of distilled water. It was found that the solubility of the above salts increased if the slurry was stirred and heated at about 60°C for 10 min. The above salt slurry is then added drop by drop using a funnel to the above zeolite slurry maintaining the same temperature in one hour. This is then refluxed at 92°C ± 5°C for 24 hours. This mixture is then cooled down and washed with distilled water and filtered using a vacuum filter. The filtered cake is then dried in an oven for 12 hours at 110°C. The cake is then powdered and calcined in air in a muffle furnace at 550°C for 5 hours at a heating rate of 1.75°C /min. The catalyst sample thus obtained is then finely powdered and pressed into pellets of size 10 – 18 mesh (U.S standard sieves). The following Table gives the compositions of the salts added for each sample. The precursors used in this study were FeF₃.3H₂O (Aldrich 99.9%) and NH₄HF₂ (Aldrich 99.9%).

Table 3.2: *Composition of the salts added in the slurry for each modified sample.*

S.No	Sample	FeF₃.3H₂O	NH₄HF₃
1	Fe-ZSM-5 - 1	0.129	0.102
2	Fe-ZSM-5 - 2	0.258	0.204
3	Fe-ZSM-5 - 3	0.555	0.417
4	Fe-ZSM-5 - 4	0.813	0.615
5	Fe-ZSM-5 - 5	0.387	0.306
6	Fe-ZSM-5 - 6	0.645	0.51

3.2 Catalyst Characterization

3.2.1 Element Analysis

The composition of the catalysts was determined by the ICP- AES technique at the Materials Characterization Lab at Penn State. The main advantage of this technique is that it can simultaneously determine the cations Si, Al, Ti, Fe, Mn etc. Approximately 0.2g of the sample was fused in 1 g of lithium metaborate at 900°C. These samples were then analyzed using Leeman Labs PS3000UV inductively coupled plasma spectrophotometer having a working range of 178 – 800nm. The samples were analyzed by drawing the sample solution prepared by the lithium metaborate fusion using a pressure pump to send the sample into a nebulizer from which the sample emerged as a fine aerosol and was carried into an ionized plasma jet (7000 to 8000K). The analyte atoms were then excited to higher energy levels. Upon returning to their ground states,

characteristic radiation was emitted that was dispersed and channeled by an optical system to a series of photomultiplier tubes. By comparing the spectra thus obtained to the spectra of the standards, the elemental compositions of the samples can be calculated.

3.2.2 Surface Area Measurements

The surface area measurements were carried out using the ASAP 2010 (Accelerated Surface Area and Pore analyzer system). Prior to the analysis of the sample, the sample surface was thoroughly degassed at 400 °C in high vacuum for 12 hours. It is very important to completely degas the sample because, if the degassing is not performed or is incomplete, the total sample surface will not be available for adsorption and thus the collected data will not present a true measure of the surface area and porosity of the sample under investigation. About 0.2 g of the sample was taken in a sample tube and degassed at 400 °C under high vacuum (about 10^{-6} torr) for 12 hours. After degassing, the sample is cooled to room temperature under vacuum and then transferred for the analysis by adsorption of N₂. For all the samples N₂ adsorption – desorption isotherms were obtained at 77 K maintained by liquid nitrogen. UHP grade nitrogen and helium were used to for obtaining adsorption – desorption isotherms and for measuring the dead space. The surface area, pore volume and pore size distribution were obtained by using different P/P₀ values and applying different methods and theories. For the determination of BET surface Area, 5 points from P/P₀ (relative pressure) 0.05 to 0.25 were taken into account. Total pore volumes were obtained by the volume of the gas adsorbed at P/P₀ = 0.99 or 1. BJH method was applied to calculate pore size distribution from adsorption branch of

isotherms. The average pore diameter was calculated as $4V/SA$ where V is the volume of the pore and SA is the surface area assumed to be a sphere.

3.2.3. XRD Studies

X – Ray powder diffraction analysis was done on both the modified and parent zeolite samples to examine the changes in structure, crystallinity and the lattice parameters. The XRD data was collected using a Sintag model X2 (theta – theta goniometer). The X ray source used was Cu K – alpha (1.540562Å) radiation with a Si (Li) Peltier detector at the Materials Characterization Lab in Penn State. The d – values were calculated by the *Jade 7.15* Software. The parent zeolite spectra were compared to that of the ZSM-5 spectra in the JCPDS library. The scattered intensity was carried out between 2θ of 5° and 60° degrees respectively and the crystallinity was calculated relatively by taking the crystallinity of the parent zeolite as 100%.

3.2.4 Nuclear Magnetic Resonance Spectroscopy

^{27}Al MAS NMR spectra of HZSM-5 and Fe-ZSM-5 samples were obtained on a Chemagnetics/Varian Infinity-Plus spectrometer using quadrature detection and an 11.74 T magnetic field. A 5mm DR Pencil probe was used. ^{27}Al transmitter frequency is 130.255445 MHz and referenced externally to AlCl_3 as 0 ppm. All spectra were run under single pulse excitation (SPE-MAS) magic angle spinning. Spin rate was 10.0 kHz, excitation pulse width was $\sim 1\mu\text{sec}$ and recycle delay was 1-2 sec.

3.2.5 Infrared Spectroscopy

Infrared Spectroscopy is widely used in heterogeneous catalysis. The basic principle of this technique is that a molecule can exist in a variety of rotational and vibrational energy levels and can move from one level to another by absorption/release of energy, which is equivalent to the difference in energy of the two involved levels. The absorption/emission of an electromagnetic radiation accomplishes these transitions and this forms a basis of vibrational spectroscopy. (Barrett et al., 1951). IR is generally used in determining the structure of the catalysts or determining the functional groups on a catalyst surface or finding the reaction intermediates or species responsible for surface modification. In this study, we have used IR to examine the presence of iron in the framework of the modified zeolites. The transmittance IR spectra were taken on a Perkin Elmer GX instrument with LASSER irradiation probe and the data was analyzed using the software supplied with the instrument. The sample was prepared by the sample and KBr (IR grade) in a 1:100 ratio and pressed into a pellet.

3.2.6 Studies for Acidity Determination

The determination of acidic sites exposed on the solid surface and their distribution is indispensable in understanding the catalytic properties. In this study, these studies have been conducted on the parent and modified catalysts to determine the strength of the acid sites and the total acidity and to compare the changes in acidity and the distribution of the acid sites on the modified catalysts. Microcalorimetry and

temperature programmed desorption are the most promising, facilitating the direct determination of the total acidity and distribution of the strength of acidic sites.

3.2.6.1 Microcalorimetric Studies on the Catalyst

Acidity by microcalorimetry is the most powerful technique for energetic characterization of solid surfaces and provides a direct and accurate method for the quantitative determination of the number of acid sites of different strengths. In microcalorimetry, the acid site is neutralized by reaction with a base and the heat evolved is measured by a calibrated micro calorimeter. Higher heat of neutralization indicates the presence of strong acid sites. This can be used to characterize the acid strength by correlating it with the energy distribution of the acid sites. Microcalorimetry has been used effectively to probe the acidic properties of various metal oxides and zeolite catalysts (Gregg and Sing, 1982).

Ammonia, pyridine and n-butyl amine are the probe bases commonly used in adsorption microcalorimetric measurements. Microcalorimetry is one of the best known methods for accurately measuring the differential heats of adsorption and therefore characterizing a catalyst by the energy distribution of its surface sites. It allows determination of the heat evolved during the interaction of appropriate ammonia adsorbate probe molecule from the gas phase with the acid sites on the surface of the catalyst. Microcalorimetric technique was used to determine the complete acid strength distribution analysis of microporous ZSM-5 material as well as Fe-incorporated ZSM-5 materials. Microcalorimetric studies of the adsorption of ammonia (critical diameter 0.3

nm) have been carried out using a Tian-Calvet type heat-flow microcalorimeter (C-80 model, Setaram, France). The microcalorimeter has been connected to a volumetric vacuum adsorption unit for catalyst pretreatment and probe molecule delivery. A validyne low-pressure transducer attached with vacuum system, which has been used for precise low-pressure measurement. The catalyst samples were pretreated by degassing under high vacuum (10^{-5} torr) at 450°C for four hours. about 0.1g of sample was used for each run.

The adsorption studies have been performed at 175°C to avoid physisorption of NH_3 . Differential heats of adsorption of ammonia against the catalyst coverage were obtained by measuring the heats evolved from sequential doses (aliquots) of micromole (μmol) quantities of ammonia on to the thermograms and the amounts of ammonia adsorbed from the initial and final pressures. Sequential dosing gives the differential heat curve (i.e. differential heat of NH_3 adsorption as a function of the amount of ammonia adsorbed on the catalyst), which provides reliable information about the number and strength of the acid sites on catalyst surface. These differential heat curves have been used to construct the acidity spectra of the catalyst samples by plotting the number of sites that adsorb ammonia with a given strength versus the strength of acid sites.

3.2.6.2 Temperature Programmed Desorption (TPD)

In TPD, a base is initially adsorbed on the surface of the catalyst. It is then made to desorb from a higher temperature to a lower temperature. As the bases desorb from the stronger acid sites they require more energy or high temperature than from weaker one.

The main disadvantage of TPD is that although TPD is a simple and rapid method, it has its limitation e.g. desorption even from non acidic sites is recorded and also there is possibility of diffusion limitations during the desorption of probe molecule from adsorption sites in the pores and cavities of zeolite causing the desorption at higher temperature than expected from actual acid strength of desorption sites. Thus it may be used to determine the acidity variations qualitatively than quantitatively. The acidity of the samples was measured using the Temperature Programmed Desorption (TPD). The TPD studies were done using the Micromeritics ASAP 2910 instrument. The sample was loaded in a quartz U tube wedged between two layers of quartz wool. About 0.2g of the sample was loaded in the powder form. The pretreatment of the sample was carried out by heating it to 450 °C at a rate of 10 °C/min for 1 hour. The carrier gas flow rate was 40 mL/min. The carrier gas used was helium. The temperature was cooled to 110 °C and ammonia adsorption was carried out. The NH₃ gas was set at a flow rate of 20mL/min in doses. The ammonia desorption was carried out from 110 °C to 700°C. The obtained data was analyzed by the GRAMS 32 software.

3.3 Catalyst Evaluation in Methylation Experiments

3.3.1 Feedstock Composition

About 60% of the compounds in the RCO and LCO have a naphthalene based structure. Since the most crucial step in the synthesis of 2, 6-DMN is the β selective reactions, 2-methylnaphthalene was used as a model compound to study the reaction. Mesitylene was used as a solvent for the feedstock and methanol was used as the

alkylating agent. Tridecane was used as the internal standard for the GC – FID analysis. The feedstock composition for the methylation reaction was 1:5:5 molar ratios of 2-m ethylnaphthalene, mesitylene and methanol.

3.3.2 Reactor System

A downflow fixed bed reactor system shown in the fig 3.1. The reactor tube used was a pyrex reactor tube of 1.2inch inner diameter and was 18.5 inches long. The catalyst bed height was found to be about 0.47 inches (12mm). The catalyst bed was placed in the middle of the reactor and the rest of the reactor was filled with inert borosilicate glass beads of 2mm in diameter. The reactor was fitted with a thermocouple to measure with a catalyst bed temperature. The reactor was placed in an electric tube furnace (Applied Test Systems 3210). The temperature in the furnace was controlled by digital temperature controller (Applied Test Systems, Series XT – 16). The desired temperature could be controlled by manually adjusting the temperature using the digital controller.

An HPLC pump (Alltech Series 426) was used to deliver liquid feed to the reactor. The pump calibration was verified using the volume of the liquid delivered in a specified time interval. UHP nitrogen was introduced in the system using a mass flow controller (Brooks model 5850 E). The mass flow controller calibration was also verified using an Agilent ADM 1000 digital flow meter. For each experiment, 0.3g of the catalyst particles (10-18 mesh) were used.

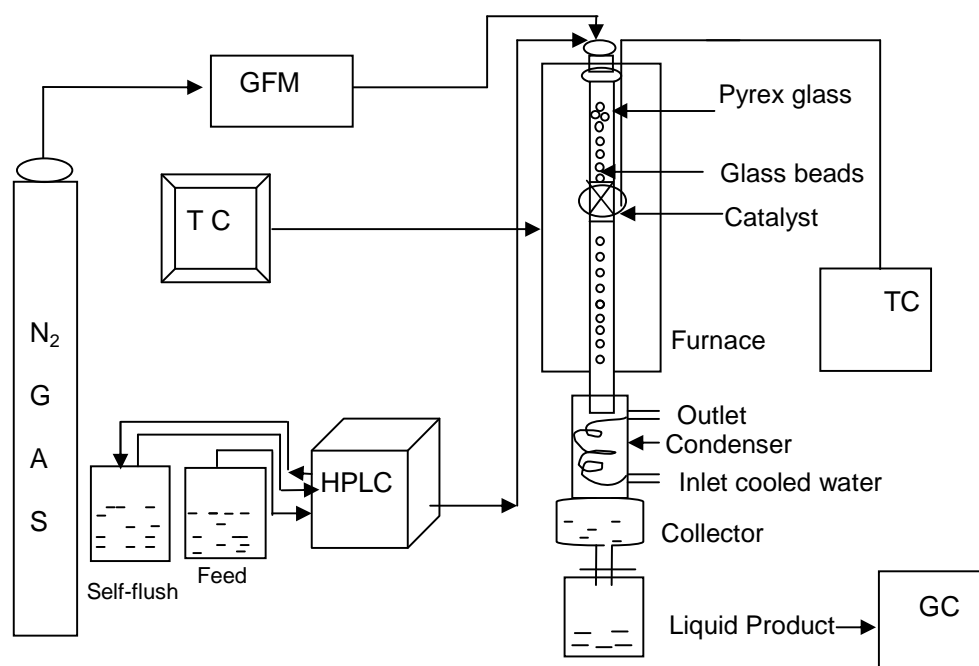


Figure 3.3.1 Schematic of the methylation reactor system.

3.3.3 Reaction Conditions

Prior to each experiment, the catalyst was pretreated by heating it to 450°C for one hour under a nitrogen flow of $20\text{mL}/\text{min}$. The temperature was increased from room temperature to 450°C at a rate of $1.8^{\circ}\text{C}/\text{min}$. The reaction was carried out at atmospheric pressure. After one hour, the temperature was reduced to the reaction temperature. The liquid feed was then introduced at a rate of $1.98\text{mL}/\text{min}$. This corresponds to a gas to liquid (G/L) ratio of 10 and a weight hourly space velocity of approximately 6.0hr^{-1} . For most of the reactions, the reaction temperature was maintained at 300°C except for the temperature dependence reactions where the reactions were carried out at 300°C , 325°C and 350°C respectively. All the reactor tubes were cleaned thoroughly and dried in an

oven over night after every reaction. A fresh and clean reactor tube was used for each experiment.

3.3.4 Sample Collection and Analysis

After the start of the HPLC pump, samples were collected every one hour for 6 hours after which the experiment was terminated. The samples collected were weighed and approximately 10 wt% Tridecane was added as the internal standard before analyzing the samples. The products were analyzed by HP 5890 GC – FID gas chromatography (GC - FID) with a β -Dex 120 capillary column having a 60m \times 0.25 mm I.D. column with 0.25 μ m coating film thickness. The split ratio was around 120. The temperature program used was as follows: The furnace was heated to 150°C before injecting the sample. About 0.4 μ L of the sample was introduced for each run. The temperature cycle was from 150°C to 180°C at a rate of 2.5°C /min.

A series of three standards were prepared and analyzed to determine the detector response factors. The response factors for the individual compounds were calculated as:

$$Rf_i = (A_i/wt_i) * (wt_{IS}/A_{IS}) * (MW_i/MW_{IS})$$

Where A is the peak area,

wt is the weight of the compound in the standard (g)

MW is the molecular weight of the compound (g/mol).

The final response factor was taken as the average of the three analyses.

The conversion of 2-MN was determined as :

$$X_{2\text{-MN}} = (n_{2\text{-MN}(f)} - n_{2\text{-MN}(p)}) / n_{2\text{-MN}(f)}$$

Where $n_{2\text{-MN}}$ = the amount of 2-MN (mol) in the feed

The ratio of 2, 6-DMN /2, 7-DMN was determined as

$$2, 6\text{-DMN}/2, 7\text{-DMN} = n_{2, 6\text{-DMN}} / n_{2, 7\text{-DMN}}$$

Where n_i (mol %) = $(A_i/A_{IS}) * n_{IS} * (1/Rf_i)$.

Chapter 4

Results and Discussion

This work deals with ZSM-5 catalyzed shape selective methylation of methyl naphthalenes for the synthesis of 2, 6-dimethylnaphthalene (2, 6-DMN). Literature studies and preliminary reactions determined that medium pore zeolites exhibited shape selectivity towards the 2, 6-DMN. This study was done as an attempt to further increase the shape selectivity of the medium pore catalysts towards the desired 2, 6-DMN molecule. It was hypothesized that the isomorphous substitution of Al in the zeolitic framework with Fe can result in a better selectivity towards the desired product. The modified catalysts were studied using several characterization techniques to determine the structural changes, the acidity changes and were evaluated for the methylation reaction. It was hypothesized that the isomorphous substitution Fe would cause partial dealumination thus lowering the acidity. The increase in either a, b or c of parameters could cause a lattice expansion. This suggests a slight pore expansion in the modified samples. A reduction in the catalyst acidity along with surface neutralization is observed in the catalyst samples. The yield of the desired compound was found to increase from 40% to about 60% using Fe modified catalysts. The 2, 6-DMN/2, 7-DMN ratio also increased from 1.7 to 2.0 for the modified catalysts.

4.1 Preliminary Methylation Reactions with Zeolites

Preliminary experiments for the methylation of methyl naphthalene were carried out on both large pore and medium pore zeolites based on the literature study. H Mordenite (CBV – 90A) and H Y zeolite (CBV – 720A) were chosen for large pore zeolites. Two types of ZSM-5 catalysts, (CBV - 5524G and CBV – 8014) were chosen amongst the medium pore zeolites. These catalysts were selected to study their activity and to determine whether the catalysts exhibited product or transition shape selective properties as reported in literature.

4.1.1 Effect of Catalyst Type on the Reaction

In order to determine the effect of the type of zeolite on the methylation, experiments were carried out using the three different types of zeolites viz. large pore zeolites (Mordenite), Faujasite type zeolite (Y Zeolite) and the medium pore MFI type zeolite (ZSM-5). As mentioned in chapter 3, all these zeolites were converted to the protonated H^+ form from the NH_4^+ form prior to the reactions. The reactions were conducted at 300°C.

The activity of the three catalysts (HY, HM and H ZSM-5 (50)) based on the 2-MN conversion for the methylation reaction is shown in the Figure 4.1. The conversion data for the first one hour might not be accurate as the timer was started as soon as the feed pump was switched on. The conversion for the large pore zeolites viz. H-Y and H-M was higher than that of HZSM-5 (50) as observed in the literature (Pu and Inui, 1996). We can observe a linear deactivation in the HY zeolite whereas in mordenite, the activity

gradually decreases over the 6 hours. The 2-MN conversion for ZSM-5 was the lowest of the three catalysts. On the other hand, the 2, 6-DMN/2, 7-DMN ratio of ZSM-5 is about 1.7 compared to a 2, 6-DMN/2, 7-DMN ratio of about 1.2 for both the large pore catalysts as shown in Figure 4.2. The pore diameters for both Mordenite ($7.0\text{\AA} \times 6.5\text{\AA}$) and Zeolite Y (7.4\AA) are larger than the critical diameters of the DMN isomers. So all the products formed effectively pass through the pores of Mordenite and Y Zeolite. In ZSM-5 ($5.6 \times 5.3\text{\AA}$ for the sinusoidal pore), the diffusion of the products through smaller pore diameter imposes certain steric restrictions on the DMN molecules. Based on the frontier molecular orbital theory (Song et al., 2000), it was reported that the HOMO of the position 6 was higher than that of position 7 for 2-MN, the formation of the 2, 6-DMN isomer is more favored compared to the 2, 7-DMN isomer thus exhibiting the electronic transition state selectivity. Additionally, the 2, 6-DMN molecule was found to be slightly linear compared to the 2, 7-DMN molecule thus aiding in easier diffusion of the isomer.

The Table 4.1 shows the 2, 6-DMN, 2, 7-DMN and all the other secondary isomerization product yields (i.e 1, 6-DMN, 1, 3-DMN, 1, 4-DMN, 1, 2-DMN, 1, 8-DMN, 2, 3-DMN) of the reactions run at 300°C . Based on the yields of the DMN isomers for the methylation reaction, it can be seen that though H Y and H M did not exhibit any kind of shape selectivity owing to its large pore sizes the 2, 6-DMN/2, 7-DMN ratio was reported to be above the equilibrium value. On the other hand, both HZSM-5 (50) and H ZSM-5 (80) have exhibited a higher yield of β , β -DMNs and a considerably higher 2, 6-DMN / 2, 7-DMN ratio of about 1.65 and 1.7. At the same time, there is a large amount of secondary isomerization taking place on the catalyst. In spite of the slight acidity

difference of the H ZSM-5 (50) and H ZSM-5 (80) catalysts, the DMN product yield and the 2, 6-DMN/2, 7-DMN ratios are also similar.

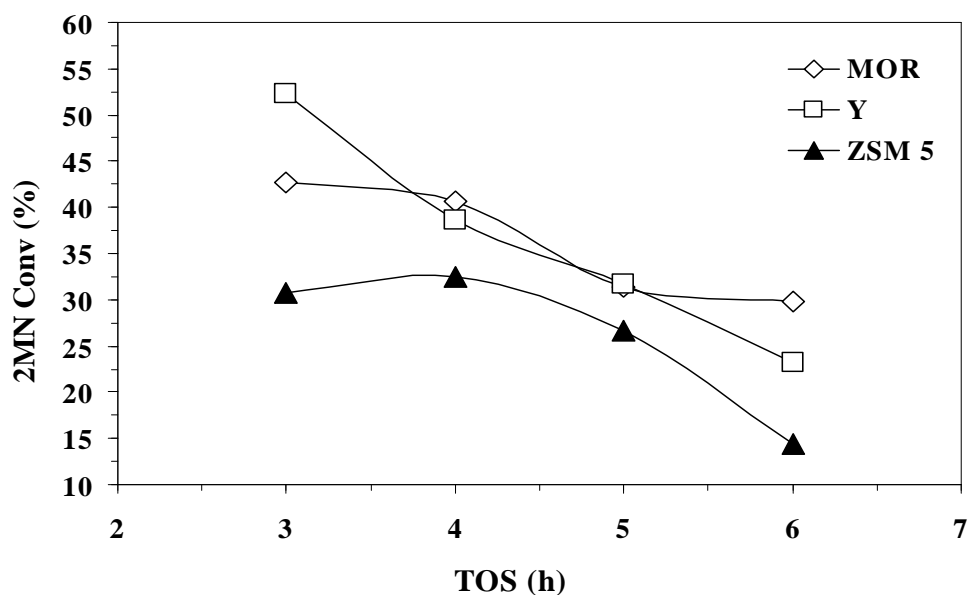


Figure 4.1: Conversion Vs TOS for the methylation of 2-MN at 300 at $6.0h^{-1}$ WHSV.

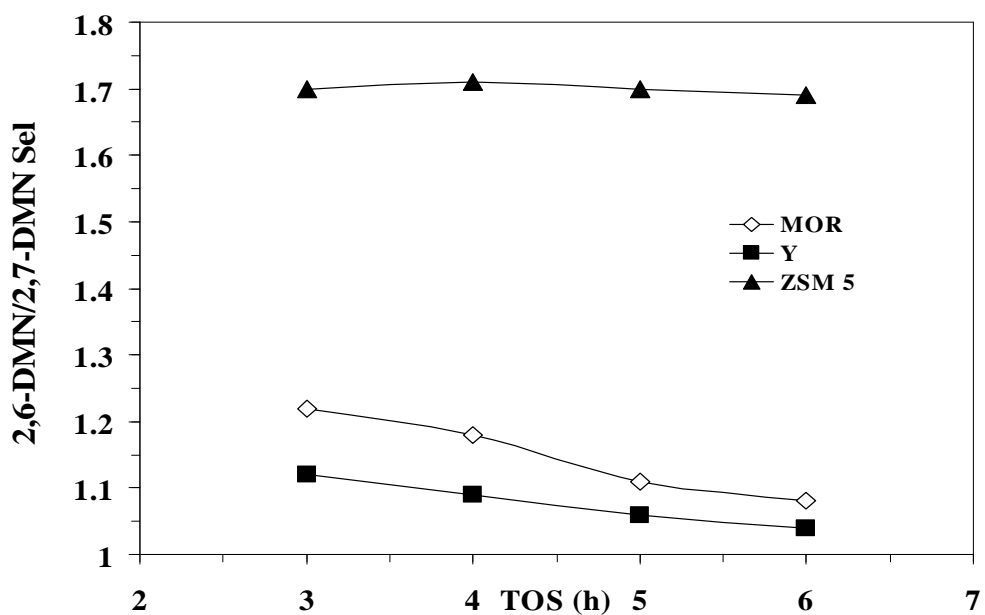


Figure 4.2: Selectivity Vs TOS for the methylation of 2-MN at 300°C at $6.0h^{-1}$ WHSV.

Table 4.1 The DMN product distribution of the 2-MN methylation reaction at 300°C and 6.0h⁻¹ WHSV. (a = Pu and Inui, 1996)

DMN Isomer	Distribution (%)				
	Thermodynamic Equilibrium	HY	HM	HZSM-5(50)	HZSM-5(80)
1, 7 -DMN	14.7	10	10.7	7.3	5.33
2, 7-DMN	11.7	32	25.9	26.2	20.8
1, 3-DMN	14.8	4.3	2.3	3.6	2.4
2, 6-DMN	12.0	36	30.3	47.2	36.4
1, 6-DMN	14.0	6.15	6.7	15.9	19
2, 3-DMN + 1, 4-DMN	(12.5 + 5)	3.3	8.3	6.1	7.4
1, 2-DMN	9.7	1.6	0	2.4	9.5
1, 8-DMN	0	6.4	1.9	0	1.9

Reaction Conditions: WHSV=6.0h⁻¹, Temperature=300°C, wt. of catalyst=0.3g

4.1.2 Effect of Temperature on the Reaction

The main objective of this study is to determine the effects of the temperature on the activity of the catalyst for the methylation reaction and the selectivity of the formation of 2, 6 dimethylnaphthalene to the 2, 7-dimethylnaphthalene compound. The experiments were conducted at 300°C, 325°C, 350°C on the H ZSM-5 (50) (CBV 5524G), catalyst samples. The Figure 4.3 shows the variation of the catalyst activity based on the 2-MN conversion with temperature. It can be observed that the activity of the catalyst was considerably lower at 300 °C compared to the activity of the reactions conducted at 325°C and 350 °C reaction. Since the feed components are 1:5:5 2-MN: Methanol: Mesitylene, there is a possibility of the conversion of the methanol to light hydrocarbons on the catalyst surface. At lower temperatures, the catalyst pores may be blocked with the side reaction products (secondary isomerization products) that are large molecules. However at higher temperatures, these molecules tend to diffuse away from the catalytic sites faster thus enabling more reactants to approach the active centers of the catalyst (Fraenkel et al., 1986).

The Figure 4.4 shows the variation of 2, 6-DMN/2, 7-DMN ratio with temperature. The selectivity however increased at lower temperatures as the conversion decreased because in most of the diffusion controlled reactions, the selectivity varies inversely with the conversion, at higher conversion rates, the rate of formation of products is high but these products tend to sit on the active sites and pore opening thus preventing the shape selective action of the zeolite.

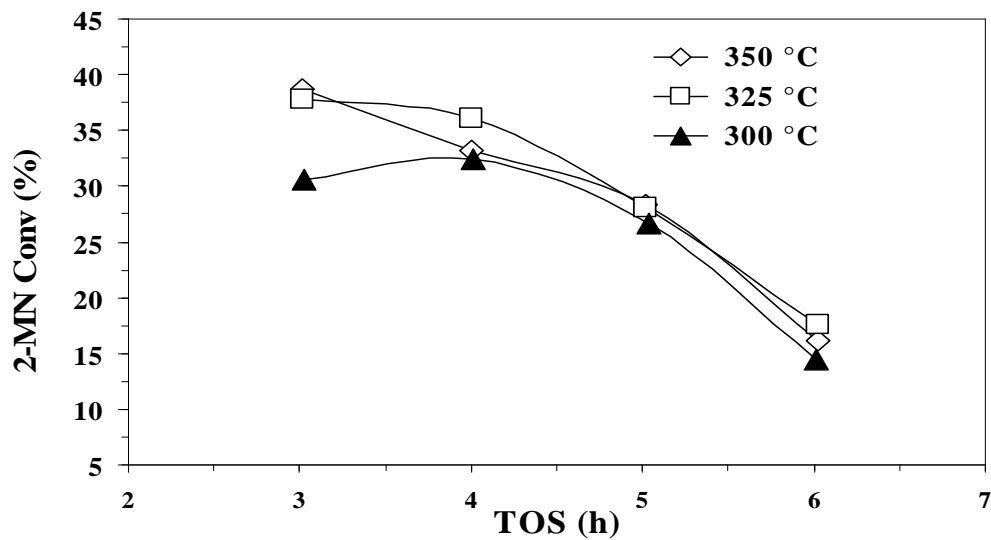


Figure 4.3: Conversion Vs TOS for the methylation of 2-MN using CBV 5524G as a catalyst at $6.0h^{-1}$ WHSV.

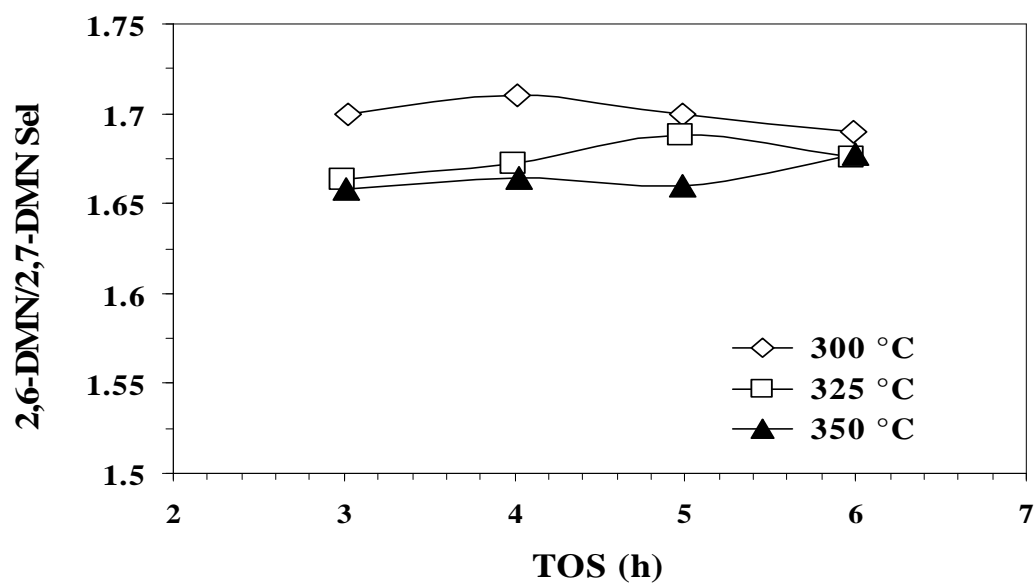


Figure 4.4: Selectivity Vs TOS for the methylation of 2-MN using CBV 5524G as a catalyst at $6.0h^{-1}$ WHSV.

4.1.3 Effect of SiO₂/Al₂O₃ Ratio on the Methylation Reaction

The methylation of 2-MN was carried out at 300°C for 6hrs TOS using two catalysts H ZSM-5 (50) and H ZSM-5 (80). The conversion and selectivity data are compared in the Figures 4.5 and 4.6 .It may be observed that the conversion of the reaction was slightly higher in the case of HZSM-5 (50) but the 2, 6-DMN/ 2, 7-DMN ratio was very close. The high conversion might be due to the higher acidity of the H ZSM-5 (50) compared to the H ZSM-5 (80) catalyst. The higher acidity promotes conversion. Thus the presence of more number of acid sites might increase the conversion levels. The 2, 6-DMN/2, 7-DMN ratio was around 1.75 for both HZSM-5 (50) than in H ZSM-5 (80) though the selectivity for HZSM-5 (50) was relatively higher than that of HZSM-5 (80). The slightly higher selectivity in the HZSM-5 (50) sample might be due to the increase in the Al content of the sample and a greater possibility in bimolecular reactions. (Mathew et al., 2001). However the difference in the respective activities and 2, 6-DMN selectivities is more or less in the same range and hence it may be concluded that since both the catalysts fall in the moderate acidity range, there is no significant difference in the performance of the two catalysts.

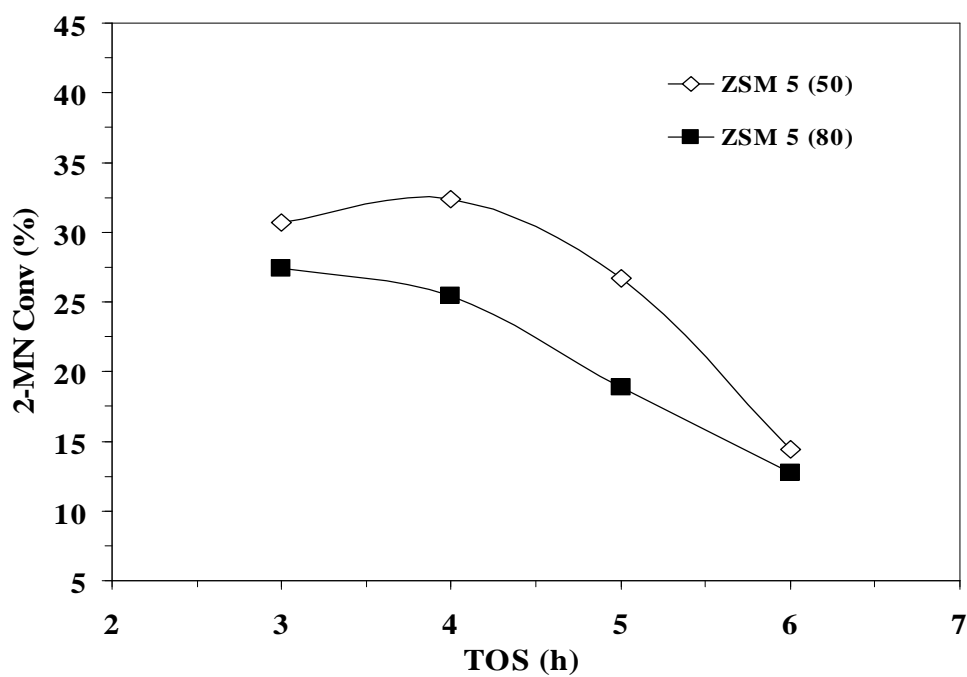


Figure 4.5 Conversion Vs TOS for the methylation of 2-MN at 300°C at 6.0h⁻¹ WHSV

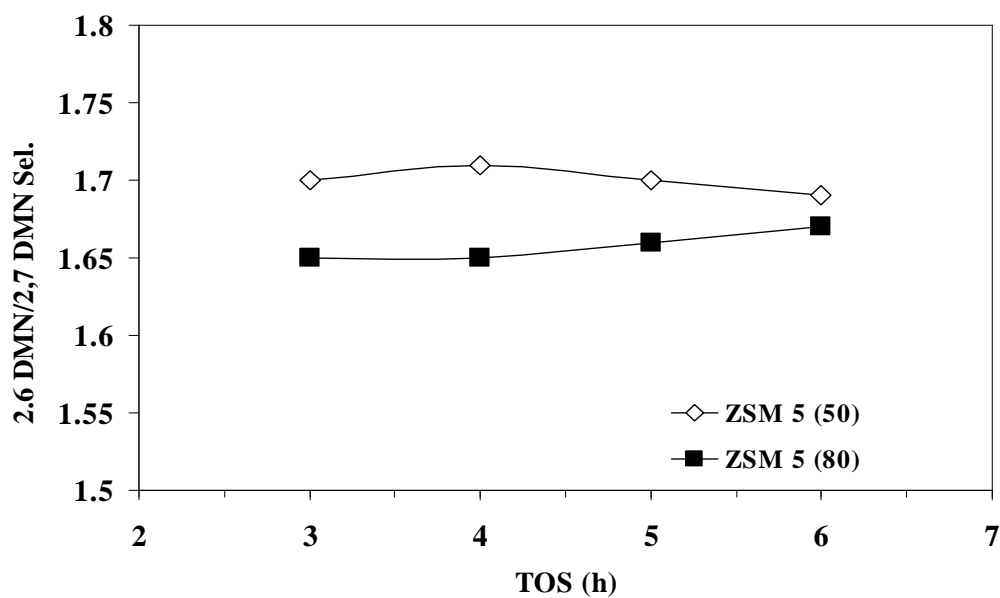


Figure 4.6: Selectivity Vs TOS for the methylation of 2-MN at 300°C at 6.0h⁻¹ WHSV

4.2 Catalyst Characterization

4.2.1 Element Analysis by ICP -AES

The chemical composition analysis of the parent and the modified samples were done by ICP AES technique. The instrument used was Leeman Labs PS3000UV inductively coupled plasma spectrophotometer. The samples were prepared by fusion of the samples in lithium metaborate. The chemical composition of the samples is given in the following Table 4.2. In order to test the accuracy of the results, the sample Fe-ZSM-5 2 was done twice and the error was about 4%. The dealumination was the highest for the samples Fe-ZSM-5 2 and Fe-ZSM-5 8. This means that the isomorphous substitution of Fe in the zeolite worked only for a certain range of Fe beyond which it decreased. The Fe/Al ratio varied from 0.23 to 1.83. In order to test the accuracy of the results, the sample Fe-ZSM-5 2 was done twice and the error was about 4%. The dealumination was the highest for the samples Fe-ZSM-5 2 and Fe-ZSM-5 8. This means that the isomorphous substitution of Fe in the zeolite worked only for a certain range of Fe beyond which it decreased. The Fe/Al ratio varied from 0.2 to 1.8.

Table 4.2: Chemical Composition of the catalyst samples before and after modification

S.No	Sample	Fe ₂ O ₃ (experiment)	Fe ₂ O ₃ (Analyzed)	Al ₂ O ₃ (wt%)	Fe/Al Ratio (wt/wt)	SiO ₂ (wt%)	SiO ₂ /Al ₂ O ₃
1	HZSM5(50)	0	<0.2	2.85	0	90	55.5
2	FeZSM5(1)	0.41	0.4	2.33	0.17	91	69
3	FeZSM5(7)	0.645	0.71	1.76	0.53	91	87
4	FeZSM5(2)	0.86	0.91	1.68	0.71	91	93
5	FeZSM5(2r)	0.86	0.94	1.61	0.77	91	95
6	FeZSM5 (8)	1.29	1.24	1.67	0.97	91	89
7	FeZSM5 (3)	1.85	1.74	1.75	1.3	89	97
8	FeZSM5 (4)	2.4	2.45	1.77	1.8	91	91

4.2.2 X-Ray Diffraction Studies

The X-Ray diffraction patterns of the different catalysts were carried out on the parent H ZSM-5 catalysts as well as the ones that were modified with Fe. The X-ray diffraction patterns were recorded using a Philips X'pert Pro powder diffractometer system with Cu K alpha (1.540560 \AA) radiation with a 0.02° step size and 1s step time.

The samples were analyzed on an as received basis without any prior pretreatment. The X-ray Diffraction patterns of the different samples were measured between 2° to $60^\circ 2\theta$. The relative crystallinities were determined considering the crystallinity of the H ZSM-5 sample as 100%.

The figure 4.7 shows the XRD patterns of the HZSM-5 samples and the Fe modified ZSM-5 samples. It may be observed that all the samples have very similar XRD patterns including all of the major peaks at the diffraction angles of $2\theta = 7.90^\circ$ and 23° are obtained. In the modified peaks, the intensities of the main peaks have increased thus indicating that the modification process brings about a slight increase in the crystallinity. It is observed that there is a relative increase in the crystallinity of the sample. The relative crystallinities were calculated by taking the crystallinity of the ZSM-5 sample as 100%. The Table 4.2 shows the relative crystallinities and the lattice parameters calculated. The crystal structure was revealed to be the orthorhombic structure. It can be seen from the above Table that there is an increase in the “*a*” axis after the modification of the HZSM-5 (50) zeolite was modified with iron. The ZSM-5 zeolite framework constitutes of two intersecting channel systems – a sinusoidal channel running parallel to the 001 indices and the other running parallel to the 010 indices. Usually, the “*a*” axis is the zigzag or sinusoidal channel of the HZSM-5, which has a significant effect on the shape selective properties of the catalysts. It can be observed that as the Fe loadings increase a axis expansion also increases. This expansion of the “*a* axis” dimensions might be attributed to the replacement of the Al in the framework by the Fe. In the Figure 4.7 below, the XRD spectra of H ZSM-5(50) and Fe-ZSM-5 were compared. It

can be seen that the relative crystallinity increased on Fe loading. The possible incorporation of the Fe in the framework also is also backed up by the fact that the acidity of the samples is significantly lowered compared to that of the parent zeolite.

Table 4.3: *Crystallinity and lattice parameters of the samples*

Sample	Description	C _{XR}	Lattice parameters		
			a	b	c
HZSM-5	CBV 5524G	100	20.1219	19.7236	13.4261
Fe-ZSM-5 1	0.4 wt % Fe	107	20.1886	19.9637	13.2896
Fe-ZSM-5 7	0.645 wt % Fe	109	20.3191	20.0531	13.2964
Fe-ZSM-5 2	0.86 wt % Fe	110	20.2072	19.9706	13.3663
Fe-ZSM-5 8	0.1.29wt % Fe	108	20.3134	20.0179	13.2721
Fe-ZSM-5 3	1.85 wt % Fe	106	20.0741	19.7726	13.4928

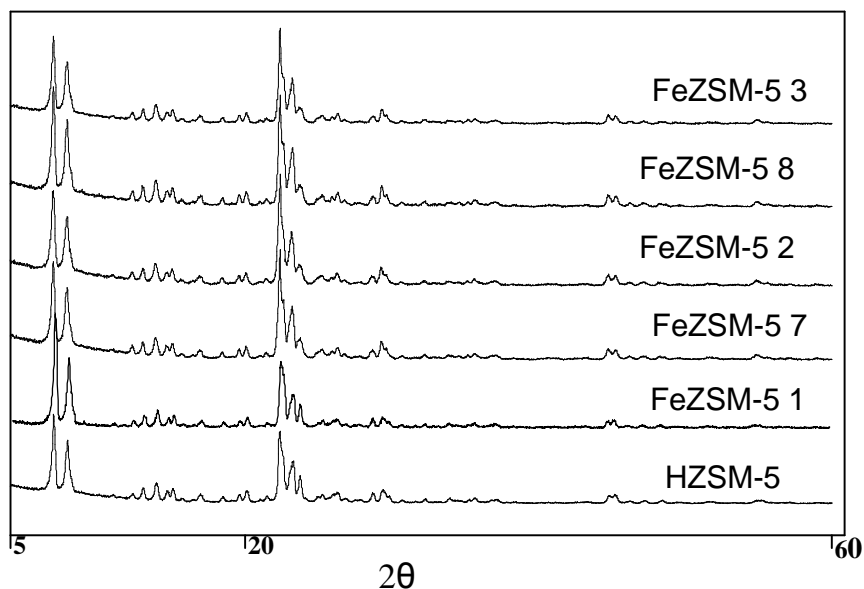


Figure 4.7 XRD Profiles of parent and modified samples

4.2.3 Surface Area Measurements

The possible incorporation of the Fe in the framework also is also backed up by the fact that the acidity of the samples is significantly lowered compared to that of the parent. The surface area and the pore size distribution were determined by BET analysis. It was also hypothesized that dealumination of the zeolite increases the activity of the catalysts thus playing a major role in the increase in conversion of 2-MN to 2, 6-DMN. It has also been hypothesized that as the Fe content in the catalyst increases, the conversion and the selectivity of the catalyst rise to a maximum and then decrease as the Fe content increases beyond that limit. The Table 4.3 shows the surface area and the pore size distribution of the samples, the surface area of the samples has definitely decreased with the increase of the Fe Content. The surface area and pore size distribution analyses were carried out on a static high vacuum volumetric unit Micromeritics ASAP 2010. The

sample was pretreated by passing Nitrogen at 350 deg C under vacuum for 12 hours. The following Table 4.4 shows the surface area and pore size distribution for Iron modified ZSM-5 containing ascending order of iron concentrations and compared with the parent HZSM-5. The total surface area was measured by the BET surface area method and the pore size was determined from the Horvath - Kawazoe method. All the other samples Fe modified samples have increasing weight percent of iron loaded. By observing the data in the Table below, we can observe, there is an overall decrease in the micro pore area as the iron loading increases. This might be attributed to some of the zeolite structure collapsing during the modification process. There is a minor variation in the pore diameter. Only one sample Fe-ZSM-5 2 shows an increase in the pore diameter. It may be suggested that during modification, the pore size increases initially reaches a maximum and then gradually decreases almost settling down close to the original pore size of the parent zeolite.

Table 4.4 Surface Area data for the modified samples

S.No	Sample	Micropore Volume	TSA(m ² /g)	Micropore Area	Mesopore Area	Pore dia (Å)
1	H ZSM-5	0.127	443	315	128.27	5.0
2	Fe-ZSM-5 1	0.11	453	279	174	4.73
3	Fe-ZSM-5 7	0.071	418	163	255	4.84
4	Fe-ZSM-5 2	0.068	412	155	257	5.13
5	Fe-ZSM-5 8	0.072	410	163	246	4.9
6	Fe-ZSM-5 3	0.063	400	144	256	4.9
7	Fe-ZSM-5 4	0.078	410	183	225	4.9

4.2.4 Infrared Spectroscopic Studies

Framework IR studies have been carried out on both parent zeolite samples and the modified catalyst samples to verify the presence in the framework of the modified samples. It has been hypothesized that isomorphous substitution of iron into a zeolite (H ZSM-5 in this case) would cause a change in acidity. In addition, the incorporation of Fe into the zeolite ion would probably cause a pore expansion bringing a modification of the catalysts selective behavior. The following figure 4.12 shows the comparison of the profiles of the modified and the parent zeolite to verify the presence of Fe ions in the framework of the ZSM-5. The IR spectra were taken in the region from 400cm^{-1} to 4000cm^{-1} . Characteristically ZSM-5 exhibits two bands one at 1100cm^{-1} and the other one around at 820 to 780cm^{-1} . The presence of Fe in the framework causes the bands to shift towards the lower frequency region compared with the absorption band of the parent zeolite. The band around the 1100cm^{-1} identifies the asymmetric vibrations of the internal tetrahedral where as the symmetric stretching of the T-O-T (Where T = Al, Si or Fe etc) is found 820 to 780cm^{-1} . The shift to the lower frequency region is due to the longer Fe – O bond compared to the Al-O bond distance. This shift to a lower frequency in the spectra can also be verified by the increase in the lattice parameters of the modified Fe-ZSM-5 samples.

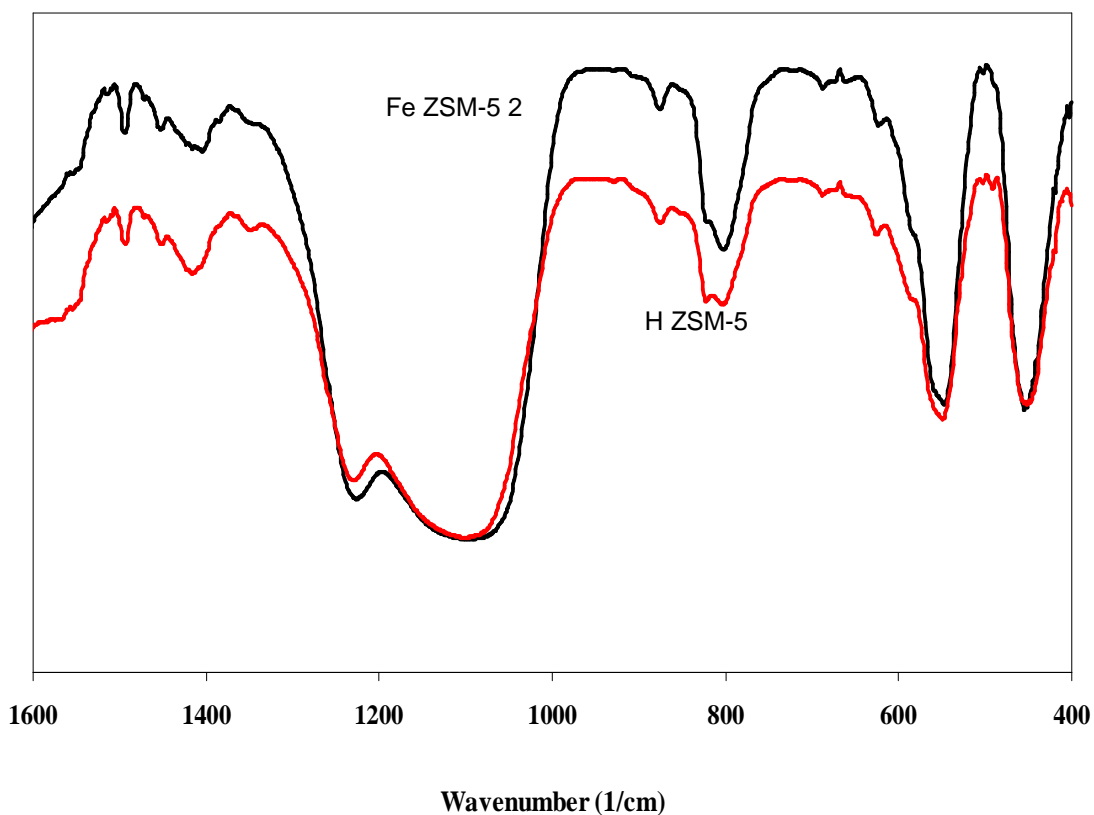


Figure 4.8: Framework IR spectra of the HZSM-5 and Fe-ZSM-5 2 samples

4.2.5 Al²⁷ MAS NMR Studies

The Al²⁷ Magic Angle Spin spectra were recorded on the parent HZSM-5 zeolite as well as the samples modified with Fe. The following figure compares the Al²⁷ NMR spectra for all the samples. We can observe two bands at 55 ppm and 0 ppm respectively in the HZSM-5 spectra. The band at 55 ppm corresponds to the tetrahedrally coordinated alumina whereas the band at 0 ppm corresponds to the octahedral coordinated alumina which is present as the external framework species (Marturano et al., 2000). The intensity of the NMR resonance bands is expected to decrease compared to the parent HZSM-5 as observed in the Figure 4.14 This might be attributed to the presence of the iron species in

close proximity of the aluminum ion species. Marturano et al.,2000,have attributed this decrease in intensity to the fact that the iron species have unpaired electrons that generate a magnetic field that creates interference in the resonance of Al nuclei.

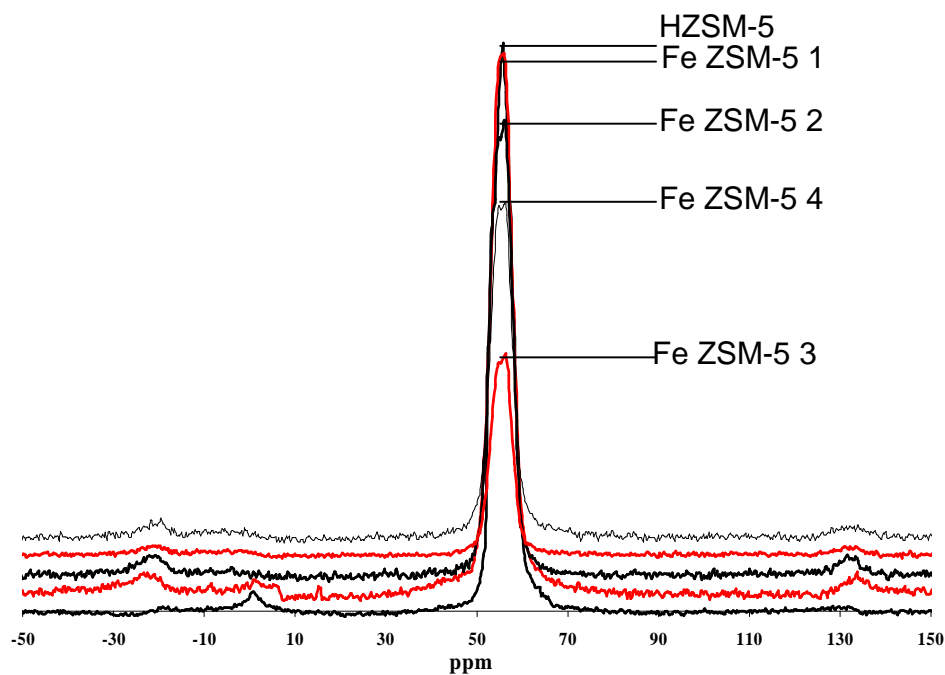


Figure 4.9: ^{27}Al MAS NMR for the parent and modified Zeolites

The presence of bands around 135 and -20ppm in the modified samples are caused because of the dipolar attraction between the electron spin of the Fe species and the Al nuclei. Krishna et al., (2006) proposed that these bands support the presence of Fe^{3+} species or other FeO_x species at the framework substitution positions. However, no information can be obtained on the type of the species present. The presence of Fe_2O_3 in the modified samples determined by the elemental analysis supports the above theory.

4.2.6 Acidity Measurements

Two kinds of acidity studies were done on the parent zeolite and the modified zeolites to determine the effect of acidity changes in the catalysts. One technique was the temperature programmed desorption of ammonia and the other was microcalorimetric studies on the absorption of ammonia.

4.2.6.1 Temperature Programmed Desorption (TPD) using NH_3 as a probe molecule

NH_3 -TPD can be used to determine the shift of peak temperature. The shift of peak temperature indicates a change in the acid strength of the samples. It is very important to have a moisture trap before the gas is sent to the TPD instrument as the presence of moisture can shift the acid site peaks as shown in the Figure 4.10. The following Figure 4.11 shows the TPD profiles of the catalyst samples and the temperatures of the two peaks are listed in the following Table 4.5. It can be seen that the parent zeolite HZSM-5 exhibits strong acid strength. The acid strength of the modified samples has decreased as shown by a shift towards the lower temperature. It may also be seen that for the sample Fe-ZSM-5 2, the peak shift for the weak acid peaks is not that high as compared to the rest of the samples. Also the sample Fe-ZSM-5 4 has a higher acidity. This has also been confirmed by the data obtained by the microcalorimetric measurements of the sample. This might be the reason that the conversion and 2, 6 - /2, 7-DMN ratio data for this sample is closer to that of HZSM-5. Also, the sample Fe-ZSM-5 3 has the least acidity of all the samples. The low activity and selectivity of the catalyst

towards the formation of 2, 6-DMN suggests that there has been a lot of dealumination. The peak at 55 ppm in Al²⁷ NMR also shows the intensity of the peak to be very low. The addition of higher amounts of Fe in the samples during modification decreases the acidity of the samples. The weakening of the strong acid sites is evident in the temperature shift towards the lower temperature.

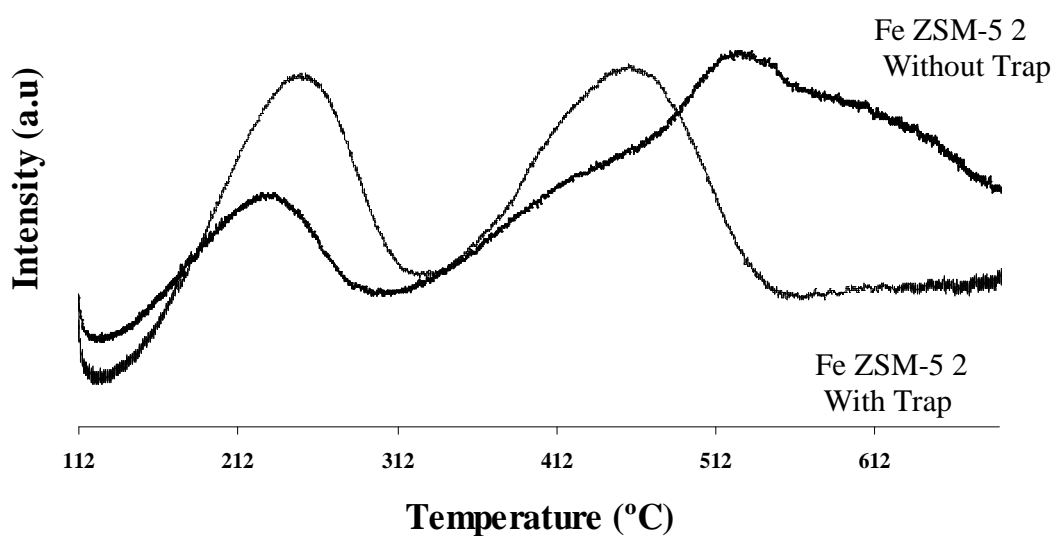


Figure 4.10 *NH₃-TPD profiles of Fe ZSM-5 2 in presence/ absence of moisture trap*

Table 4.5 *Temperatures at the TPD peaks shown in the Figure 4.11.*

Sample	Low temperature	High temperature
HZSM-5	260	494
Fe-ZSM-5 1	251	459
Fe-ZSM-5 2	256	458
Fe-ZSM-5 3	238	440
Fe-ZSM-5 4	252	460

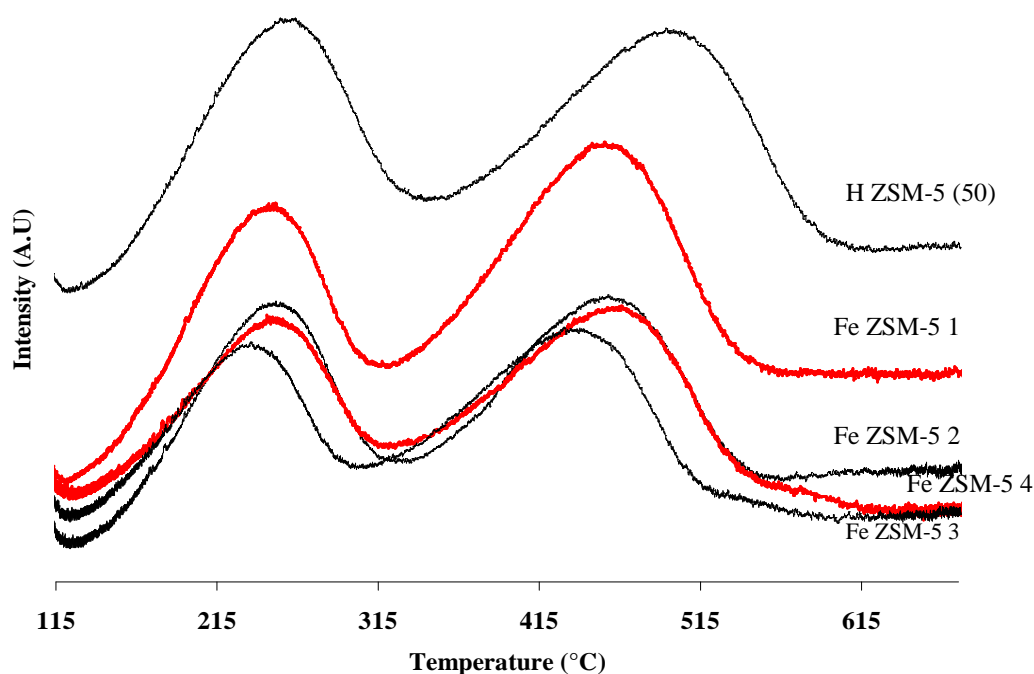


Figure 4.11: TPD profiles of Parent and modified catalyst samples

4.2.6.2 Microcalorimetric Studies

This technique provides the quantitative information about the number and the strength of the acid sites on the samples. The Table 4.6 below lists out the acidity distribution of the acid sites in the parent zeolite and the iron modified zeolites. The acid sites are classified into strong, weak and medium acid sites. The strong acid sites are identified as sites which have a heat of adsorption more than 100kJ/mol. The sites between 80 kJ/mol and 100 kJ/mol are classified as medium acid sites. The sites having heats of adsorption below 80 kJ/mol are the weak acid sites.

Table 4.6 Acid strength distribution of parent and modified zeolites

S.No.	Catalyst Samples	Total Acidity (mmol/g)	Acid Strength Distribution*			Initial Heats (kJ/mol)
			S	M	W	
1.	H-ZSM-5	0.823	0.485	0.140	0.313	120.62
2.	Fe-ZSM-5 1	0.759	0.325	0.115	0.319	141.65
3.	Fe-ZSM-5 7	0.559	0.245	0.105	0.209	131.58
4.	Fe-ZSM-5 2	0.518	0.265	0.065	0.188	134.31
5.	Fe-ZSM-5 8	0.545	0.250	0.095	0.200	126.09
6	Fe-ZSM-5 3	0.396	0.17	0.085	0.141	137.04
7	Fe-ZSM-5 4	0.603	0.210	0.175	0.158	140.08

The microcalorimetric adsorption pattern of ammonia and the resulting enthalpy of adsorption as a function of the volume of ammonia adsorbed over ZSM-5 samples are given in the Figure 4.12. It can be seen that ammonia interacted with these sites in a heterogeneous manner. In this case, the heat of adsorption varied in the wide range between 140 to 40 kJ/mol. A steep slope of the Q values at low coverage indicates the presence of very strong lewis acid sites as in the Fe-ZSM-5 3 sample. The formation of a plateau of constant heats of absorption of NH₃ on the H ZSM-5 sample indicates the presence of bronsted acid sites (Brindusa et al., 2004). It is observed that the heat of adsorption decreased with coverage in well defined steps, in all of the samples. This

systematic decrease of the differential heats observed in the present case is due to the interaction of ammonia with a variety of the surface sites that exhibit different strengths. The curves become steeper with the increase in the iron concentration in the samples. This shows the dealumination in these samples.

The TPD data as previously mentioned also concurred with the above data showing that there is a decrease in the acid strength. Figure 4.13 gives the acid strength spectra of all of the samples. In this plot, the distribution of acid strengths i.e. dn/dq vs. the heats of absorption Q . We can see that as the iron content of the samples increased, there is a distinct shift of the strong acid sites towards the medium acid sites. It may be observed that the sample Fe-ZSM-5 2 particularly has a higher concentration of medium acid sites compared to the rest of the modified samples and the parent sample. The shift of the strong acid sites towards higher Q values might be due to the presence of some extra framework aluminum species as revealed in NMR studies discussed in the following sections. Thus as the Fe quantities increased, we can see a significant change in the acidity of the samples. The presence of more medium acid sites in the Fe-ZSM-5 2 might be the reason for the higher selectivity of the samples as weak acidity favors the selectivity towards 2, 6-DMN.

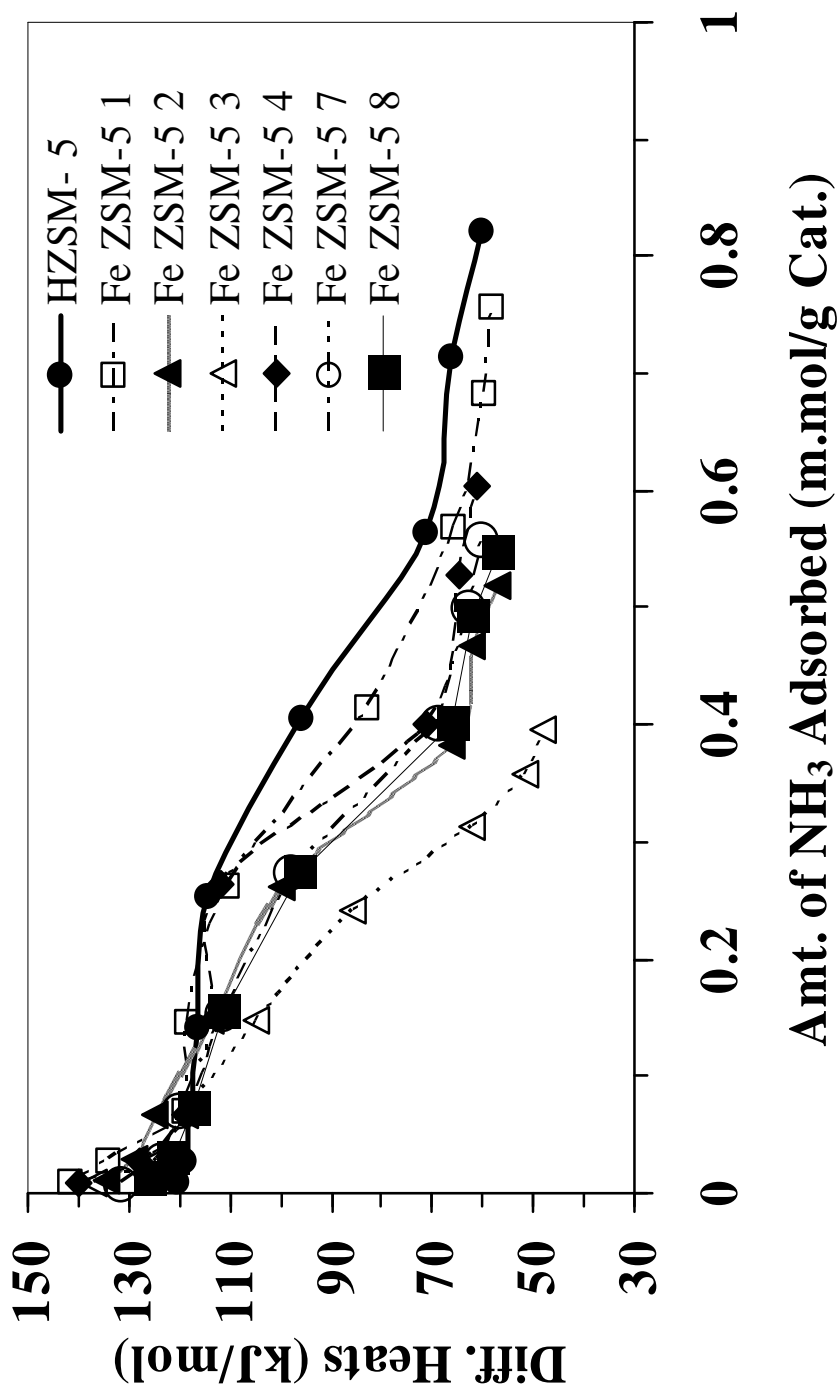


Figure 4.12: Differential Heats Distribution of all the Catalyst Samples

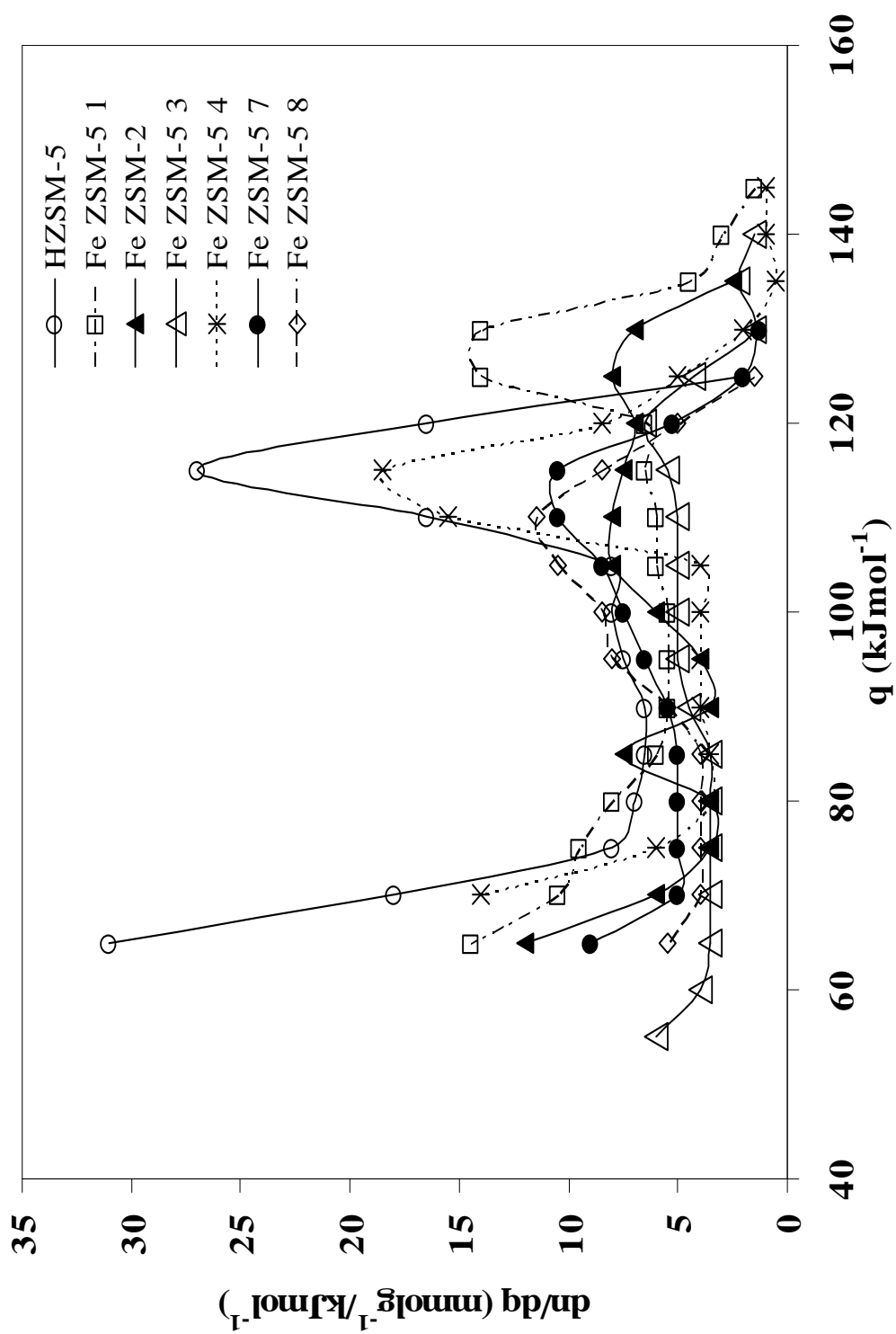


Figure 4.13 Acidity spectra of the modified samples.

4.3 Effect of Catalyst Modification on the Methylation Reaction

The methylation was carried on the modified HZSM-5 (50). The zeolites were modified by the framework substitution of Al with Fe. About six different catalysts with different Fe loadings were prepared using the isomorphous substitution method and catalytically tested at 300°C using the same experimental conditions as that for the parent zeolite H ZSM-5 (50). It was hypothesized that the incorporation of Fe in the zeolite framework would shape selectively improve the yield of 2, 6-DMN. Also, the modification process would cause neutralization of the surface sites thus inhibiting secondary isomerization reactions on the surface. The Figure 4.14 shows the 2-MN conversion with Time on stream (TOS) for H ZSM-5 and the modified samples Fe-ZSM-5 1 to Fe-ZSM-5 4. Based on the experimental results in Figure 4.14 below, we can observe a decrease in the overall catalyst activity for the modified catalyst compared to HZSM-5 activity. This dip in the 2-MN conversion was expected as the modification of the catalysts also kills some of the external surface active sites.

The Figure 4.15 shows the selectivity of the catalysts towards the 2,6 DMN. While it is clear that the overall selectivity of the catalyst towards 2, 6-DMN has increased, upon modification, the highest selectivity was obtained for the catalyst Fe-ZSM-5 2. Though the acidity of the Fe-ZSM-5 3 sample is lower than Fe-ZSM-5 2 sample, we can see that its activity and selectivity were lower. To further evaluate the effect of acidity modification on the catalyst activity two more samples (Fe-ZSM-5 7 and Fe-ZSM-5 8). The sample Fe-ZSM-5 7 was chosen with the Fe content higher than Fe-ZSM-5 1 and less than Fe-ZSM-5 2. The sample Fe-ZSM-5 8 was chosen for its Fe content less than

Fe-ZSM-5 3. The Figures 4.16 and 4.17 show the catalyst performance in terms of activity and selectivity for these two catalysts and compared against Fe – ZSM-5 2 sample. We can observe that there is not much difference between the results obtained on the catalyst Fe-ZSM-5 2 and these samples though the selectivity was slightly higher for the sample Fe-ZSM-5 2. Though it is evident that the overall acidity decreased due to the modification, based on the methylation experiment results, we can say that the increase in selectivity is valid only for a certain acidity range (around 0.54 mmol/g of catalyst). The DMN distribution in the products of the methylation reactions on the modified samples is listed in the Table 4.7. Based on the yield, we see that though the 2, 6-DMN yields have increased, there is only a slight increase in the 2, 7-DMN yield. Also, comparing the yield to the parent ZSM-5 (50) (Table 4.1), we can see that the overall yield of non selective isomers has decreased upon the catalyst modification possibly due to the surface site neutralization during modification. The parent HZSM-5 (50) exhibits very strong acid strength compared to the modified catalysts. When the ZSM-5 is modified by Fe, both the population of acid sites and the acid strength are reduced as can be observed in the following sections showing the NH₃-TPD data and the microcalorimetric studies. Komatsu et al., (2000) proposed that the alkylation reactions are usually catalyzed by weak acid sites.

Also, it can be seen that the 2, 7-DMN yield only increases slightly though the 2, 6-DMN yield has almost doubled for the modified catalysts. This could be because of the shape selective properties of the catalysts. Komatsu et al., (2000) reported that the selective formation of 2, 6-DMN might be due to product selectivity. The recent

computational studies done by Song et al., (2000) report that the critical diameters of the 2, 6-DMN and 2, 7-DMN are same at 7.19Å. The studies further show that the electron density in the highest occupied molecular orbital (HOMO) is a measure of the reactivity of the molecule at the specific position. In the case of 2-MN methylation they reported that the electron density at the C-6 position higher than at the C-7 position. Thus the formation of the 2, 6-DMN isomer is more favorable inspite of the similar critical diameters. It can be said that the 2, 6 – DMN formation exhibits the electronic state shape selectivity.

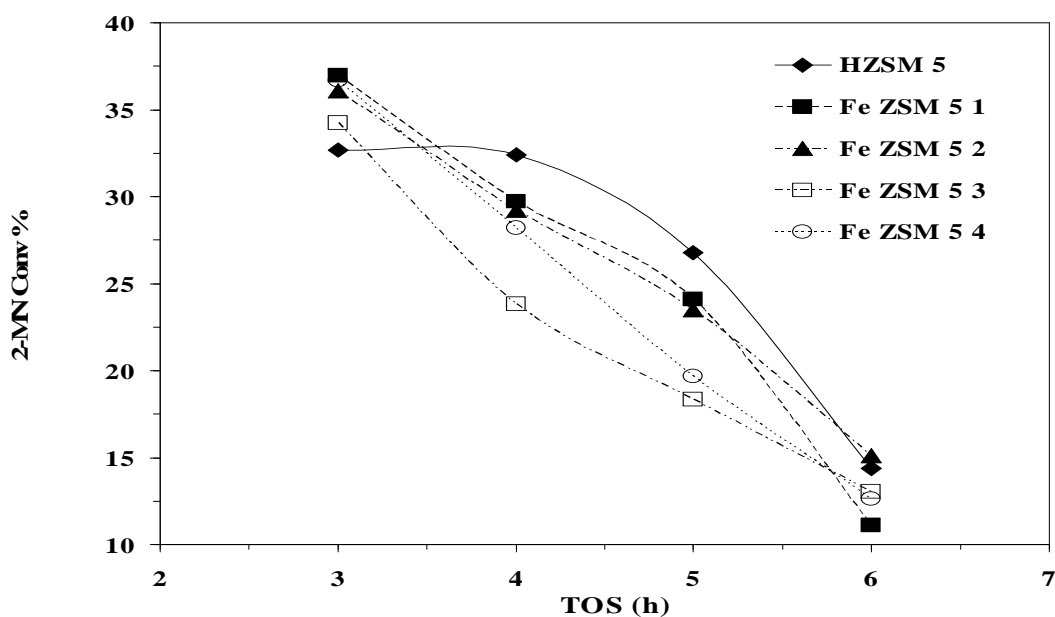


Figure 4.14 2 MN Conversion vs. TOS for the methylation of 2-MN at 300°C at 6.0h⁻¹ WHSV

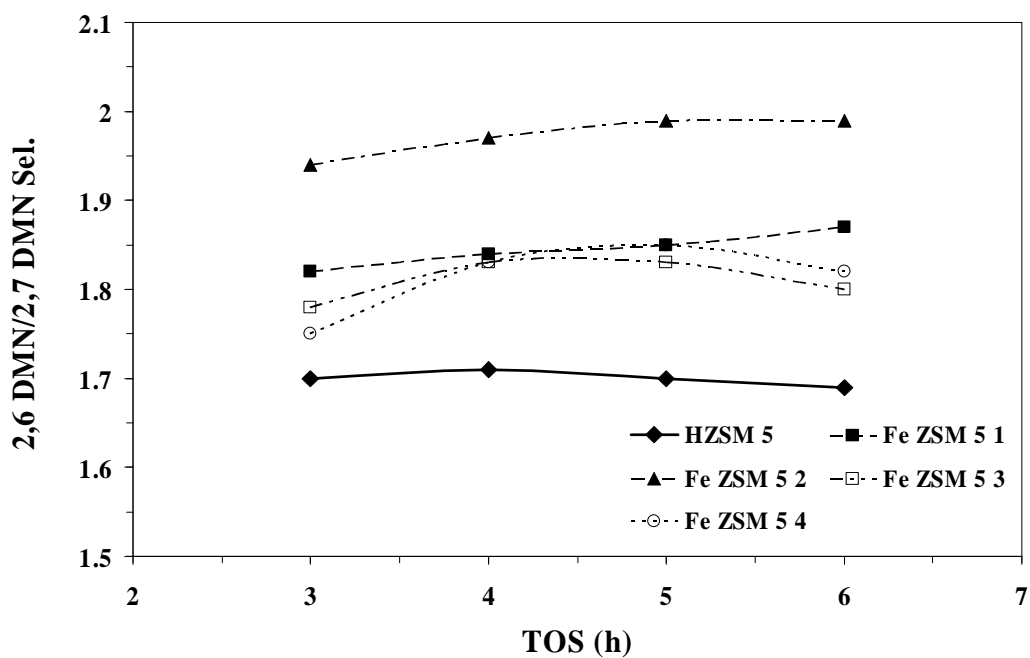


Figure 4.15: Selectivity Vs TOS for the methylation of 2-MN at 300°C at 6.0h⁻¹ WHSV

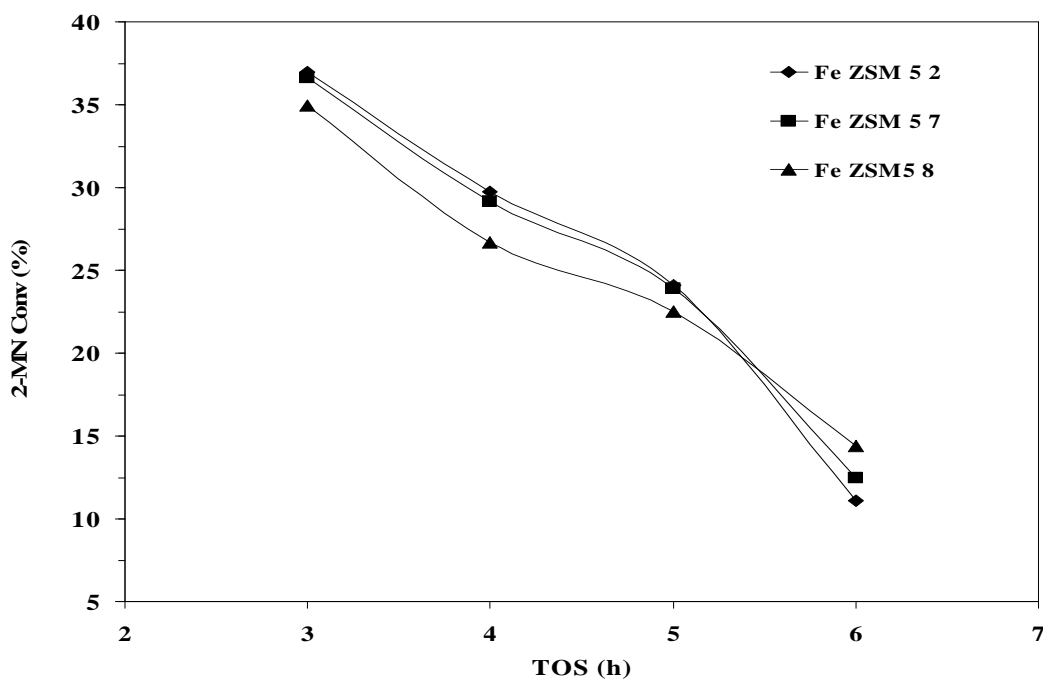


Figure 4.16: 2 MN Conversion vs. TOS for the methylation of 2-MN at 300°C at 6.0h⁻¹ WHSV

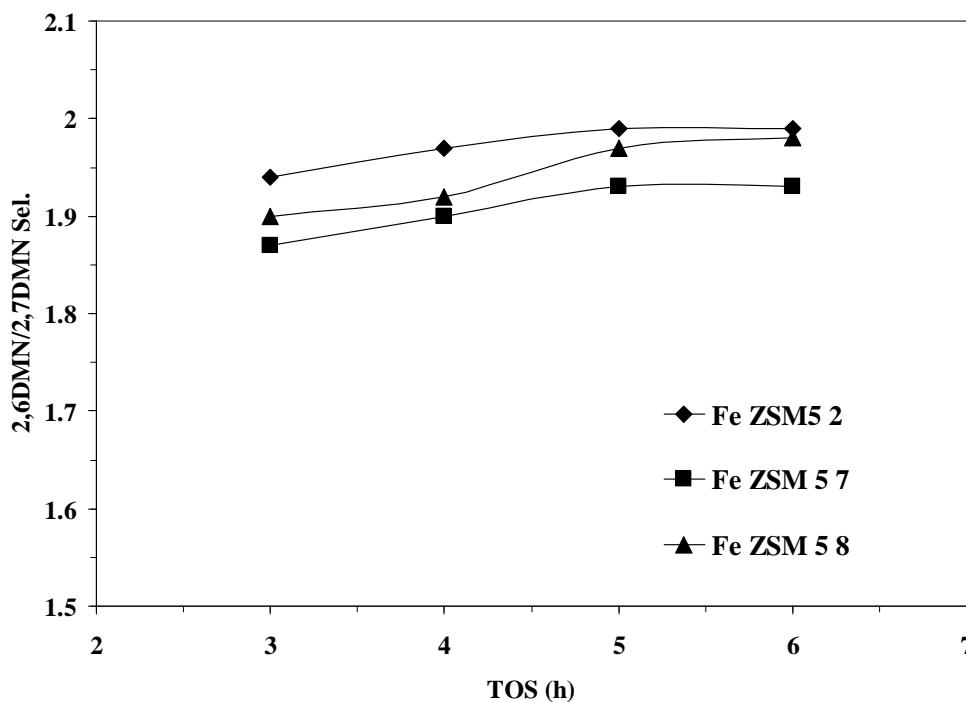


Figure 4.17: Selectivity Vs TOS for the methylation of 2-MN at 300°C at 6.0h⁻¹ WHSV

Table 4.7 Product Distribution of the DMN's during the methylation reaction conducted using the Fe-modified catalysts.

DMN Isomer	Thermodynamic Equilibrium	Distribution (%) Fe-ZSM-5 (*)					
		(*) = 1	7	2	8	3	4
1,7-DMN	14.7	14	17.8	3	1	2.7	3.75
2,7-DMN	11.7	25	29.6	23.21	27.7	30.1	33.1
1,3-DMN	14.8	7	0	0	0	0	0
2,6-DMN	12.0	46	58.6	45	49.9	57.5	62.1
1,6-DMN	14.0	3.1	0	0	0	0	0
2,3 + 1,4-DMNs	(12.5 + 5)	0	0	20.9	5.2	8.5	2.5
1,2-DMN	9.7	0	0	0	0	1	0
1,8-DMN	0	4.2	0	7	14.6	0	0

Reaction Conditions: WHSV=6.0h⁻¹, Temperature=300°C, wt. of catalyst=0.3g

The isomorphous substitution of Fe in the framework of the zeolite caused a slight lattice expansion confirmed by the XRD and pore size distribution results discussed in previous sections which may aid the diffusion of the 2, 6-DMN molecule. This slight stretching of the pore channels might bring about a reduction in the diffusional constraints otherwise brought about when using H ZSM-5 as a catalyst.

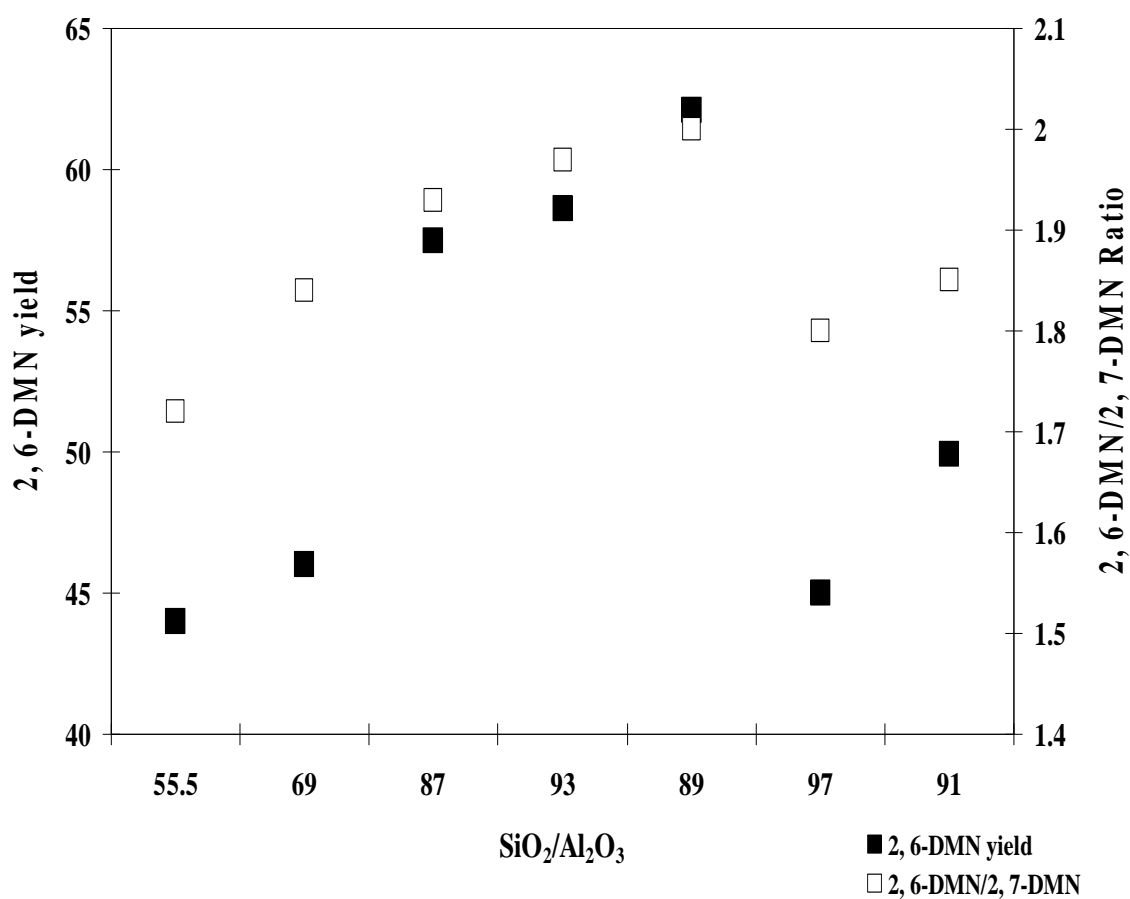


Figure 4.18 Trend for the 2, 6-DMN yield and 2, 6-DMN/2, 7-DMN ratio for the methylation experiments

Table 4.8 2, 6 DMN yield distribution for for methylation experiments

Sample	2, 6-DMN Yield	2, 7-DMN Yield	2,6/2,7-DMN Ratio	SiO₂/Al₂O₃
H ZSM-5(50)	36	21	1.72	55.5
Fe ZSM-5 1	46	25	1.84	69
Fe ZSM-5 7	58	30	1.93	87
Fe ZSM-5 2	59	30	1.99	93
Fe ZSM-5 8	62	30	1.97	89
Fe ZSM-5 3	45	25	1.8	97
Fe ZSM-5 4	50	27	1.85	91

The Figure 4.18 shows the 2, 6-DMN yield and 2, 6-DMN/2, 7-DMN ratio plotted against the SiO₂/Al₂O₃ ratio of the modified catalysts given in the Table 4.8. We can observe that though the 2, 6-DMN yield and the 2, 6/2, 7-DMN ratio increased after modification, no clear trend is observed with the increase in the dealumination i.e increase in the SiO₂/Al₂O₃. Thus it may be concluded that the isomorphous substitution of the medium pore zeolite sample with Fe has definitely aided the formation of 2, 6-DMN as compared to the 2, 7-DMN isomer while effectively inhibiting a lot of the other β isomers.

4.4 Experimental Uncertainty

A series of three duplicate experiments were conducted to determine the experimental uncertainty. The results are shown in the figures (4.18 and 4.19) and the Tables (4.7 and 4.8) and the conversions of the duplicate are represented as the same symbols (Filled and unfilled). In order to quantify the error, the raw data is presented in the Table. The average of the absolute value of all the differences in the corresponding data or both the conversion and the 2, 6-DMN/2, 7-DMN ratio were taken. Those points where the selectivity was same were not considered. The uncertainty among the duplicates sets of conversion was calculated to be approximately $\pm 2\%$ and that for the 2, 6-DMN/2, 7-DMN was found to be 0.02.

Thus the conversions for all the experiments can be taken as approximately $\pm 2\%$ and the 2, 6-DMN/2, 7-DMN ratios as approximately ± 0.02 . Care was taken not to make judgements about the performance of catalysts whose conversion and the 2, 6 - DMN/2, 7-DMN ratio fell within those ranges of uncertainty.

Table 4.9 Raw data for 2, 6-DMN/2, 7-DMN ratio for the three sets of duplicate experiments

	H ZSM-5 (80)		H ZSM-5 (50)		Fe-ZSM-5 1	
TOS (h)	A	B	C	D	E	F
1	78.35	72.87	77.85	76.56	76.41	77.33
2	41.81	38.66	48.50	47.03	45.08	42.84
3	28.74	27.43	30.7	31.36	32.71	33.97
4	24.44	25.41	32.41	31.16	29.1	29.7
5	17.98	18.95	28.73	26.46	19.1	17.93
6	13.9	12.7	14.32	12.61	10.69	11.12

Table 4.10 Raw data for 2, 6-DMN/2, 7-DMN ratio for the three sets of duplicate experiments

	H ZSM-5 (80)		H ZSM-5 (50)		Fe-ZSM-5 1	
TOS (h)	A	B	C	D	E	F
1	1.62	1.59	1.62	1.6	1.67	1.69
2	1.67	1.64	1.68	1.68	1.79	1.77
3	1.66	1.65	1.7	1.71	1.81	1.81
4	1.66	1.65	1.71	1.73	1.83	1.85
5	1.67	1.66	1.7	1.72	1.85	1.85
6	1.69	1.67	1.69	1.7	1.89	1.87

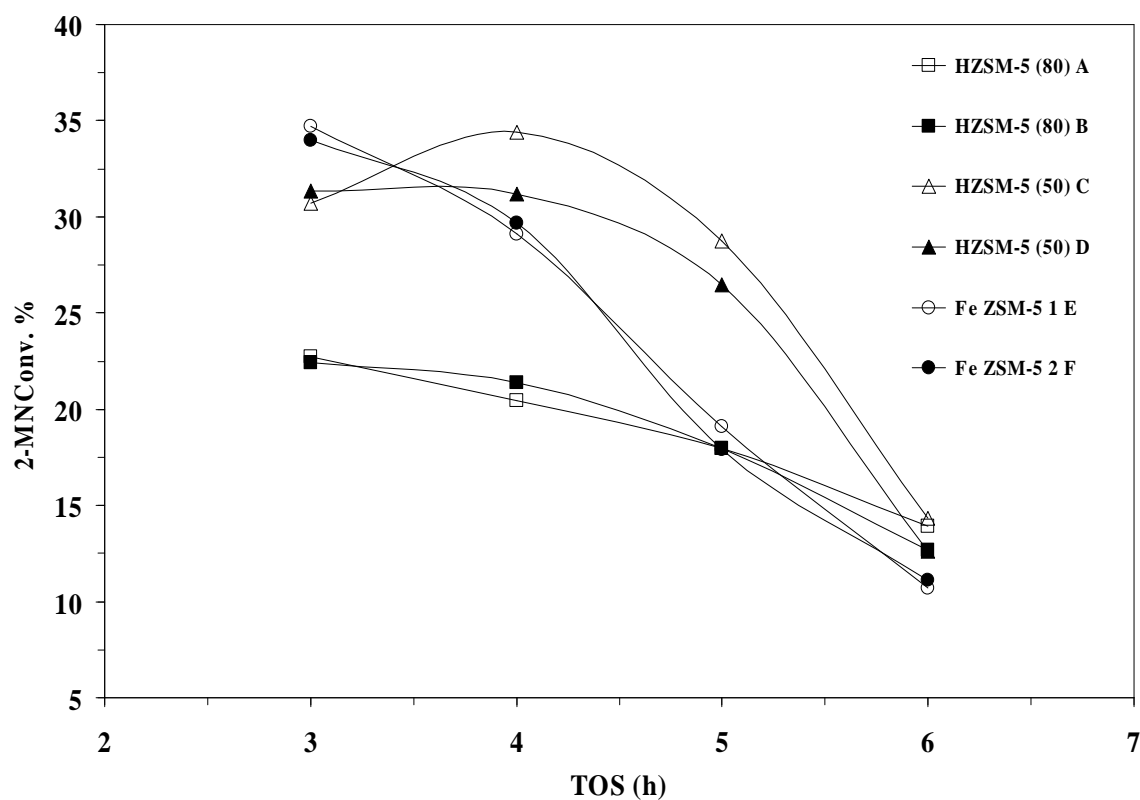


Figure 4.19 Conversion Vs TOS for three sets of duplicate experiments

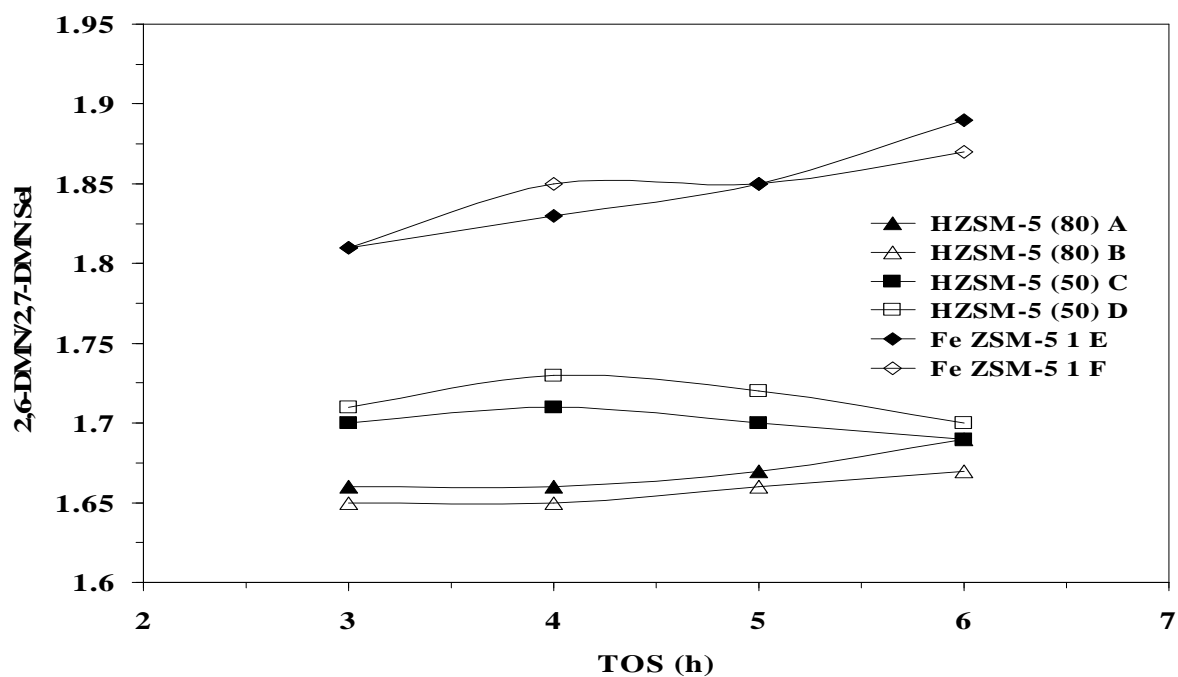


Figure 4.20 2, 6-DMN/2, 7-DMN vs TOS (h) for three sets of duplicate experiments

Chapter 5

Summary, Conclusions and Recommendations for Future Work

5.1 Summary

Based on the results of the experiments conducted for the methylation of 2-MN to get 2, 6-DMN various zeolite based catalysts prepared for this study and the consequent characterization of those catalysts, the following results were obtained:

- ZSM-5 is the best zeolite for the methylation of methyl naphthalene to get 2, 6 dimethylnaphthalene based on the present conditions.
- A lower $\text{SiO}_2/\text{Al}_2\text{O}_3$ ratio also favors the formation of 2, 6-DMN
- The modified catalysts show an increase in the 2, 6 DMN/2, 7 DMN ratios.
- The 2, 6-DMN/2, 7-DMN ratio is around 2 for the sample Fe-ZSM-5 2.
- Addition of Fe to the zeolite also stabilized the deactivation of the catalyst for a longer time.
- As the Fe content of the samples increased, the 2, 6-DMN/2, 7 -DMN ratio was lowered.

- Based on the acidity experiments conducted the highest catalyst performance was when the acidity was around 0.5 mmol/g. Also, acidity was lowered significantly on addition of Fe.
- The higher performance of the Fe-ZSM-5 2 sample can be attributed to the presence of higher number of medium acid sites in the zeolites as opposed to more number of strong acid sites on the HZSM-5.
- XRD studies show that no structural changes have been observed before and after modification. There is a slight increase in the crystallinity of the zeolites after modification and the lattice parameters have also increased.
- The IR and NMR studies reveal the presence of Fe in the framework of the zeolites.
- However the pore size variation with the modification in the zeolite is yet to be determined.

5.2 Conclusions

The following conclusions are derived:

- The performance of ZSM-5 as a catalyst for the methylation reaction can be improved through the modification of the catalyst with Fe by the isomorphous substitution method.

- The substitution of Fe in place of Al brings about an increase in the 2, 6 -/2, 7-DMN ratio at 300°C. It also gives more stability to the catalyst.
- A higher number of medium acid sites promote the selectivity and the reaction.
- The acidity around 0.5 to 0.6mmol/g may be the ideal range for the catalyst performance, based on the data obtained for the best catalysts.
- No clear trend was observed in the pore size change during modification of the zeolite.

5.3 Recommendations for Future Work

The following recommendations are proposed to further this course of study:

- The methylation reactions using modified ZSM-5 catalysts modified by the isomorphous substitution of other metals like Ga, Ti etc. should also be carried out and the effect of their structural changes on the shape selectivity towards the 2, 6-dimethylnaphthalene isomer should also be determined. It is also recommended that a mixture of large pore and medium pore zeolites should be used as the catalyst and the effect on the 2, 6-DMN yield should also be determined.
- A careful study of the effects of calcination temperature on the zeolite structure and the modification process is strongly recommended. The effect of the calcination temperature on the metal-zeolite framework coordination during the

calcination after modification is to be studied. The use of UHP air or Oxygen cylinders is recommended in place of the hood air supply. A moisture trap installation is recommended in the air – muffle furnace tubes. A proper air flow meter is also recommended for more accurate control.

- It is recommended that a series of catalyst regenerability tests are conducted for the best Fe modified catalyst samples. The TOS for the reaction should also be further extended to about 8 hours to study the catalyst stability. The effect of feed to solvent ratio and the feed ratio should also be examined.

References

Abe T., Uchiyama S., Ojima T., Kida K., US 5,008,479 (16 April), 1991, Patent to MGC.

Allen J., Malmberg E., US 3,235,615 (15 February), 1966, Patented to Sun Oil.

Angevine P.J., Degnan T.F., Marler D.O., US 5,001,295, 1991, Patent to Mobil.

Baerlocher C., Meier W., Olsen D.H., Atlas of Zeolite Framework Types, 2001, New York, Elsevier.

Beaumont R. and Barthomeuf D., Journal of Catalysis, 1972, **27**, pp. 45.

Barrett E.P., Joyner L.G., Halenda P.P., Journal of the American Chemical Society, 1951 **73**, pp. 373.

Eberhardt G.C., Peterson H.J., Journal of Organic Chemistry, 1965, **30**, pp.82.

Eberly Jr. P.E., Kimberlin Jr C.N. and Voorhies A. Jr., Journal of Catalysis, 1971, **22**, pp.419.

Fang Y. and Hu H., Catalysis Communications, 2006, **7**, pp. 264.

Fellmann J.D., Saxton R.J, Weatrock P.R., Derouane E.G., Massiani P, US, 5026942. , 1991, Patent.

Fraenkel D., Cherinavsky M., Ittah B., and Levy M., Journal of Catalysis, 1986, **101**, pp. 273.

Gläser R., Li R., Hunger M., Ernst S., Weitkamp J., Catalysis Letters, 1998, **50**, pp.41.

Gregg S. J., Sing K. S. W., Adsorption, Surface Area and Porosity, 1982, 2nd Ed., New York.

Harad T., Kurozumi S., Nagahama S., Nishikawa T., Shimada K., Takeuchi Y., US 3,798,280 (19 March), 1974, Patented to Teijin Ltd.

Hibino T., Niwa M., Murakami Y., Journal of Catalysis, 1991, **128**, pp. 551.

Horsley JA., Fellman J.D., Derouane E.G., Freeman C.M., Journal of Catalysis, 1994, **147**, pp.231.

Inui T., Nagata H., Takeguchi T., Iwamoto S., Matsuda H., Inoue M., Journal of Catalysis, 1993, **139**, pp. 482.

Inui T., Pu S.B., Kugai J., Applied Catalysis A: General, 1996,**146**, pp. 285.

Jin L., Hu H., Wang X., Liu C., Industrial Engineering Chemistry Research, 2006, **45**, pp. 3531.

Katayama A, Toba M., Takeuchi G., Mizukami F., Niwa S., Mitamura S., Journal of Chemical Society , Chemical Communication, 1991, *Issue 1*, pp. 39.

Kim J-H., Sugi Y., Matsuzaki T., Hanaoka T., Kubota Y., Tu X., Matsumoto M., Microporous Materials, 1995, **5**, pp.113.

Kim J-H., Sugi Y., Matsuzaki T., Hanaoka T., Kubota Y., Tu X., Matsumoto M., Nakata S., Kato A., Seo G., Pak C., Applied Catalysis A: General, 1995, **131**, pp. 15.

Klein H., Fuess H., Ernst S., Weitkamp J., Microporous Materials, 1994, **3**, pp. 291.

Komatsu T., Araki Y., Namba S., Yashima T., Studies in Surface Science and Catalysis Series, 1994, **84**, pp. 1821.

Komatsu T., Kim J.H., and Yashima T. , In Shape Selective Catalysis, 2000, Song C. Garces J.M., Sugi Y., Eds., American Chemical Society ,Washington D.C, pp. 162.

Kozo T. and Holderich W., Applied Catalysis A: General, 1999, **181**, pp. 399.

Krishna K, Makkee M., Catalysis Today, 2006, 114, pp. 23.

Lillwitz L.D, Applied Catalysis A: General, 2001, 221, pp.337.

Mathew I., Mayadevi S, Sabne S, Parthy S.A., Sivasanker S.,Reaction Kinetics Catalysis Letters, 2000,**74**, pp. 119.

Marturano P., Drozdov' L., Kogelbauer A., Prins R., Journal of Catalysis, 2000, **192**, pp. 236.

Millini R.,Frigerio F.,Bellussi G., Pazzuconi G., Perego C., Pollesel P., Romano U., Journal of Catalysis, 2003, **217**, pp. 298.

Motoyuki M., Yamamoto K., McWilliams J., Bundens R., US 5,744,670, 1998, Patent to Kobe-Mobil.

Moreau P., Finiels A., Geneste P. and Solofo J., Journal of Catalysis, 1992, **136**, pp. 487.

Moreau P., Finiels A., Geneste P., Joffre J., Moreau F., Solofo J., Catalysis Today, 1996, **31**, pp. 11.

Ogata K. and Shimosato K., US 3,671,578 (20 June), 1972, Patented to Teijin Ltd.

Pu S.B., Inui T., Applied Catalysis A: General, 1996, **146**, pp. 305.

Schmitz A and Song C., Catalysis Today, 1996, 31, pp. 19.

Shen, J.-P., Song C., Sun L., presented at I&EC Symposium on Green Chemistry, American Chemical Society Spring National Meeting, Orlando, FL, April 7-11, 2002.

Silvia J.M., Ribeiro M.F., Ribeiro F.R., Gnep N.S., Guisnet M. Benazzi E., Reaction Kinetics Catalysis Letters, 1995, **54**, pp. 209.

Stienmetz G.R. and Rule M., US 4,845,273 (4 July), 1989, Patent to Eastman Kodak.

Song C., Ma X., Schmitz A.D., Schobert H.H., Applied Catalysis A: General, 1999, **182**, pp. 175.

Song C., In Shape Selective Catalysis, 2000, Song C., Garces J.M., Sugi Y., Eds., American Chemical Society, Washington D.C, pp. 248.

Song C., Ma X., Schobert H.H., In Shape Selective Catalysis, 2000, Song C., Garces J.M., Sugi Y., Eds., American Chemical Society: Washington D.C., pp.305.

Song C., Cattech, 2002, **6**, pp. 64.

Song C. and Kirby S., Microporous Materials, 1994, **2**, pp. 467.

Sumitani K. and Shimada K., JP 0413637 (17 January), 1992, Patent to Teijin Ltd.

Thomas J.M. and Lambert R.M., Characterization of Catalysts, 1980, published by Wiley Eastern and Sons.

Tustin G.C. and Rule M., Journal of Catalysis, 1994, **147**, pp. 186.

Vinek H., Derewinski M., Mirth G., Lercher J.A., Applied Catalysis, 1991, **68**, pp. 277.

Weitkamp J. and Neuber M., Studies in Surface Sciences and Catalysis Series, 1991, **60**, pp. 291.

Xu H., Song C., Zhao J., Wang L., Gan W., Acta Pet.Sin, 1999, **15**, pp. 52.

Appendix A

Standard Sample Raw Data for the Methylation Products

Two sets of standard samples were made and each sample was analyzed in the GC-FID for three consecutive runs per each sample and the average of these R.f's was taken. n-Tridecane was used as the internal standard and the GC program used was same as the one used for the analysis of the methylation experiments. The response factor was calculated using the formula:

$$\text{Internal Response Factor} = \frac{\text{Area (I.S)} \times \text{Amounts (S.C)}}{\text{Amounts (I.S)} \times \text{Area (S.C)}}$$

Where: I.S = Internal Standard

S.C = Specific compound of interest

Sample 1 - Run 1

S.No	Sample	Weight (g)	Peak Area (GC-FID)	Response Factor
1	n-tridecane	1	4485012.40	1
2	2-MN	1	4527446.90	0.98520
3	Naphthalene	0.01595	99357.77	0.716
4	1-MN	0.1156	324918.30	0.7840
5	2, 6-DMN	0.1024	673216.40	0.6788
6	2, 7-DMN	0.1195	827041.40	0.6444
7	1, 7-DMN	0.029	415489	0.3113
8	1, 3-DMN	0.01395	144065.60	0.4319
9	1, 6-DMN	0.01358	168039.60	0.3606
10	2, 3+1, 4+1, 5-DMN	0.04806	657806.20	0.3260
11	1, 2-DMN	0.01752	184662.40	0.4231
12	1, 8-DMN	0.02413	169105.20	0.636
13	1, 3, 5-TMN	0.0210	170134.10	0.5505

Sample 1 – Run 2

S.No	Sample	Weight (g)	Peak Area (GC-FID)	Response Factor
1	n-tridecane	1	4193221.40	1
2	2-MN	1	4177097.42	0.998
3	Naphthalene	0.01595	92003.03	0.7229
4	1-MN	0.1156	384918.30	0.7540
5	2, 6-DMN	0.1024	620037.80	0.6887
6	2, 7-DMN	0.1195	761519.30	0.6544
7	1, 7-DMN	0.029	382652.20	0.3161
8	1, 3-DMN	0.01395	132730.50	0.4382
9	1, 6-DMN	0.01358	154741.40	0.3660
10	2, 3+1, 4+1, 5-DMN	0.04806	606187.80	0.330
11	1, 2-DMN	0.01752	170181.40	0.429
12	1, 8-DMN	0.02413	155952.60	0.645
13	1, 3, 5-TMN	0.0210	156356.7	0.5619

Sample 1 – Run 3

S.No	Sample	Weight (g)	Peak Area (GC-FID)	Response Factor
1	n-tridecane	1	4931755.50	1
2	2-MN	1	4944511.20	0.991
3	Naphthalene	0.01595	106814.25	0.7324
4	1-MN	0.1156	364918.30	0.7340
5	2, 6-DMN	0.1024	744571.10	0.674
6	2, 7-DMN	0.1195	914870.70	0.640
7	1, 7-DMN	0.029	458610.0	0.310
8	1, 3-DMN	0.01395	159156.0	0.429
9	1, 6-DMN	0.01358	185449.20	0.3591
10	2, 3+1, 4+1, 5-DMN	0.04806	724957.60	0.3251
11	1, 2-DMN	0.01752	203354.68	0.4225
12	1, 8-DMN	0.02413	185814.10	0.636
13	1, 3, 5-TMN	0.0210	189967.60	0.544

Sample 2 – Run 1

S.No	Sample	Weight (g)	Peak Area (GC-FID)	Response Factor
1	n-tridecane	1	2074616	1
2	2-MN	1	1748269.40	1.18
3	Naphthalene	0.0159	36314.43	0.9062
4	1-MN	0.1256	324918.30	0.7340
5	2, 6-DMN	0.1124	259752.10	0.8133
6	2, 7-DMN	0.1095	319377.30	0.7720
7	1, 7-DMN	0.029	158257.60	0.3780
8	1, 3-DMN	0.01265	53485.20	0.5381
9	1, 6-DMN	0.01328	62577.50	0.4477
10	2, 3+1, 4+1, 5-DMN	0.04706	249694.00	0.3971
11	1, 2-DMN	0.01702	69103.20	0.5231
12	1, 8-DMN	0.02213	63389.50	0.7854
13	1, 3, 5-TMN	0.0210	64948.40	0.6693

Sample 2 – Run 2

S.No	Sample	Weight (g)	Peak Area (GC-FID)	Response Factor
1	n-tridecane	1	1610627	1
2	2-MN	1	1580848.60	1.0132
3	Naphthalene	0.0159	33480.69	0.7630
4	1-MN	0.1256	295699.60	0.6262
5	2, 6-DMN	0.1124	230515.60	0.71156
6	2, 7-DMN	0.1095	283469.20	0.6752
7	1, 7-DMN	0.029	140857.70	0.3297
8	1, 3-DMN	0.01265	47737.20	0.4680
9	1, 6-DMN	0.01328	55862.80	0.3893
10	2, 3+1, 4+1, 5-DMN	0.04706	223776.60	0.3440
11	1, 2-DMN	0.01702	61990.40	0.4527
12	1, 8-DMN	0.02213	57811.10	0.6685
13	1, 3, 5-TMN	0.0210	5781.80	0.5830

Sample 2 – Run 3

S.No	Sample	Weight (g)	Peak Area (GC-FID)	Response Factor
1	n-tridecane	1	2235381	1
2	2-MN	1	1980903.1	1.1284
3	Naphthalene	0.0159	41388.76	0.8567
4	1-MN	0.1256	369324.40	0.6958
5	2, 6-DMN	0.1124	292467	0.7783
6	2, 7-DMN	0.1095	259354.20	0.7392
7	1, 7-DMN	0.029	178598.80	0.3609
8	1, 3-DMN	0.01265	60553.00	0.5121
9	1, 6-DMN	0.01328	70806.60	0.4263
10	2, 3+1, 4+1, 5-DMN	0.04706	282543.40	0.3781
11	1, 2-DMN	0.01702	78216.5	0.4979
12	1, 8-DMN	0.02213	72119	0.7438
13	1, 3, 5-TMN	0.0210	73029.70	0.6414